(2)

US ARMY MATERIEL COMMAND

TECHNICAL REPORT BRL-TR-2672

A COMPUTATIONAL INVESTIGATION OF THE EFFECT OF SHIELDING IN MITIGATING SHOCK INITIATION STIMULI PRODUCED BY IMPACT

John Starkenberg
Toni M. Dorsey
Kelly J. McGlothlin

September 1985

US ARMY BALLISTIC RESEARCH LABORATORY
ABERDEEN PROVING GROUND, MARYLAND

Destroy this report when it is no longer needed.
Do not return it to the originator.

Additional copies of this report may be obtained from the National Technical Information Service, U. S. Department of Commerce, Springfield, Virginia 22161.

The findings in this report are not to be construed as an official Department of the Army position, unless so designated by other authorized documents.

The use of trade names or manufacturers' names in this report does not constitute indorsement of any commercial product.

REPORT DOCUMENTATION PAGE

READ INSTRUCTIONS BEFORE COMPLETING FORM

1. REPORT NUMBER: Technical Report BRL-TR-2672
2. GOVT ACCESSION NO.: AD-A159506
3. RECIPIENT'S CATALOG NUMBER:

4. TITLE (and Subtitle): A COMPUTATIONAL INVESTIGATION OF THE EFFECT OF SHIELDING IN MITIGATING SHOCK INITIATION STIMUI I PRODUCED BY IMPACT

5. TYPE OF REPORT & PERIOD COVERED: FINAL

6. PERFORMING ORG. REPORT NUMBER:

7. AUTHOR(s): John Starkenberg
Toni M. Dorsey
Kelly J. McGlothlin

8. CONTRACT OR GRANT NUMBER(s):

9. PERFORMING ORGANIZATION NAME AND ADDRESS: US Army Ballistic Research Laboratory
ATTN: AMXBR-TBD
Aberdeen Proving Ground, MD 21005-5066

10. PROGRAM ELEMENT, PROJECT, TASK AREA & WORK UNIT NUMBERS: 1L162618AH80

11. CONTROLLING OFFICE NAME AND ADDRESS: US Army Ballistic Research Laboratory
ATTN: AMXBR-OD-ST
Aberdeen Proving Ground, MD 21005-5066

12. REPORT DATE: September 1985

13. NUMBER OF PAGES: 58

14. MONITORING AGENCY NAME & ADDRESS (if different from Controlling Office):

15. SECURITY CLASS. (of this report): UNCLASSIFIED

15a. DECLASSIFICATION/DOWNGRADING SCHEDULE:

16. DISTRIBUTION STATEMENT (of this Report)

Approved for public release; distribution unlimited.

17. DISTRIBUTION STATEMENT (of the abstract entered in Block 20, if different from Report)

18. SUPPLEMENTARY NOTES

19. KEY WORDS (Continue on reverse side if necessary and identify by block number)

Interround Propagation, Sympathetic Detonation, Shielding, Shock Processing

the integral of p² compared with respect to t

20. ABSTRACT (Continue on reverse side if necessary and identify by block number)

We have conducted a study of the role of shielding in reducing the shock initiation stimulus for a simple one-dimensional representation of the problem of sympathetic detonation of munitions. We found that single layered shields made of materials with low acoustic impedance generally produce a complex shock wave structure in the acceptor. This complex structure is associated with a low level of initiation stimulus because of the breakup into several weaker shocks and the reduction of $\int p^2 dt$. High impedance shield materials

20. ABSTRACT (continued)

the integral of P squared with respect to t

also substantially reduce the initiation stimulus, but without the accompanying shock breakup effect. Increasing shield thickness improves performance and can change the order of effectiveness of shield materials. With multilayered shields composed of a high-impedance and a low-impedance material we observed shock structures depending strongly on the ordering of the materials in the shield. Multiple shock structure was usually observed when the high-impedance material was the outer component of the shield and sufficient low-impedance material was present. Single compression waves with variable peak pressures and rise times were usually observed when the low-impedance material was the outer component of the shield. Substantial benefits in terms of shock breakup and $\int p\,dt$ reduction can be obtained by increasing the thickness of three-layered shields, which were found to perform better than five-layered shields.

TABLE OF CONTENTS

		Page
	LIST OF ILLUSTRATIONS	5
I.	INTRODUCTION	9
II.	SIMULATION DESCRIPTION	9
III.	CHARACTERIZATION OF THE SHOCK INITIATION STIMULUS	11
IV.	RESPONSE OF UNSHIELDED ACCEPTORS	11
V.	RESULTS WITH SINGLE LAYERED SHIELDS	15
	A. General	15
	B. Shock Structure	15
	C. Initiation Stimulus Reduction	15
VI.	RESULTS WITH MULTILAYERED SHIELDS	29
	A. General	29
	B. Shock Structure	29
	C. Initiation Stimulus Reduction	41
VII.	SUMMARY	51
	DISTRIBUTION LIST	55

LIST OF ILLUSTRATIONS

Figure		Page
1	One-Dimensional Representation	10
2	Typical Acceptor Explosive Shock Pressure History without Shielding	12
3	Variation of Shock Initiation Stimulus with Wall Thickness in the Absence of Shielding	13
4	Correlation of Shock Initiation Stimulus with Flyer and Cover Plate Parameters	14
5a	Acceptor Explosive Pressure History with 5-mm Thick Lucite Shield	16
5b	Acceptor Explosive Pressure History with 15-mm Thick Lucite Shield	17
5c	Acceptor Explosive Pressure History with 25-mm Thick Lucite Shield	18
5d	Acceptor Explosive Pressure History with 35-mm Thick Lucite Shield	19
6a	Acceptor Explosive Pressure History with 5-mm Thick Magnesium Shield	20
6b	Acceptor Explosive Pressure History with 15-mm Thick Magnesium Shield	21
6c	Acceptor Explosive Pressure History with 25-mm Thick Magnesium Shield	22
6d	Acceptor Explosive Pressure History with 35-mm Thick Magnesium Shield	23
7a	Acceptor Explosive Pressure History with 5-mm Thick Tungsten Shield	24
7b	Acceptor Explosive Pressure History with 15-mm Thick Tungsten Shield	25
7c	Acceptor Explosive Pressure History with 25-mm Thick Tungsten Shield	26
7d	Acceptor Explosive Pressure History with 35-mm Thick Tungsten Shield	27
8	Variation of Shock Initiation Stimulus with Initial Acoustic Impedance of 30-mm Thick Shields	28

LIST OF ILLUSTRATIONS (continued)

Figure		Page
9	Variation of Shock Initiation Stimulus with Shield Thickness for Lucite, Tungsten and 304-Steel Shields	30
10a	Acceptor Explosive Pressure History with 30-mm Thick Three-Layered Tungsten/Lucite/Tungsten Shield at 8.3% Lucite . . .	31
10b	Acceptor Explosive Pressure History with 30-mm Thick Three-Layered Tungsten/Lucite/Tungsten Shield at 16.7% Lucite. . .	32
10c	Acceptor Explosive Pressure History with 30-mm Thick Three-Layered Tungsten/Lucite/Tungsten Shield at 33.3% Lucite. . .	33
10d	Acceptor Explosive Pressure History with 30-mm Thick Three-Layered Tungsten/Lucite/Tungsten Shield at 50% Lucite. . . .	34
10e	Acceptor Explosive Pressure History with 30-mm Thick Three-Layered Tungsten/Lucite/Tungsten Shield at 91.7% Lucite. . .	35
11a	Acceptor Explosive Pressure History with 30-mm Thick Three-Layered Lucite/Tungsten/Lucite Shield at 16.7% Lucite. . . .	37
11b	Acceptor Explosive Pressure History with 30-mm Thick Three-layered Lucite/Tungsten/Lucite Shield at 33.3% Lucite. . . .	38
11c	Acceptor Explosive Pressure History with 30-mm Thick Three-Layered Lucite/Tungsten/Lucite Shield at 66.7% Lucite. . . .	39
11d	Acceptor Explosive Pressure History with 30-mm Thick Three-Layered Lucite/Tungsten/Lucite Shield at 91.7% Lucite. . . .	40
12a	Acceptor Explosive Pressure History with 50% Lucite Three-Layered Tungsten/Lucite/Tungsten Shields at 15-mm Shield Thickness	42
12b	Acceptor Explosive Pressure History with 50% Lucite Three-Layered Tungsten/Lucite/Tungsten Shields at 25-mm Shield Thickness	43
12c	Acceptor Explosive Pressure History with 50% Lucite Three-Layered Tungsten/Lucite/Tungsten Shields at 35-mm Shield Thickness	44
12d	Acceptor Explosive Pressure History with 50% Lucite Three-Layered Tungsten/Lucite/Tungsten Shields at 45-mm Shield Thickness	45
13	Acceptor Explosive Pressure History with a 30-mm thick, 50% Lucite Five-Layered Tungsten/Lucite/Tungsten/Lucite/Tungsten Shield . . .	46
14	Relative Stimulus Levels for 30-mm Thick, Three-Layered Tungsten/Lucite Shields.	47
15	Relative Stimulus Levels for 30-mm Thick, Three-Layered Steel/Lucite Shields	48

LIST OF ILLUSTRATIONS (continued)

Figure		Page
16	Comparison of Relative Stimulus Levels for 30-mm Thick, Three-Layered Tungsten/Lucite and Steel/Lucite Shields	49
17	Effect of Shield Thickness on Relative Stimulus Level for Three-Layered Tungsten/Lucite/Tungsten Shields	50
18	Relative Stimulus Levels for 30-mm Thick, Five-Layered Tungsten/Lucite Shields.	52
19	Comparison of Relative Stimulus Levels for 30-mm Thick, Three-Layered and Five-Layered, Tungsten/Lucite Shields.	53
20	Effect of Shield Configuration on Relative Stimulus Level for 33.3% Lucite, Three-Layered and Five-Layered Shields	54

I. INTRODUCTION

In order to reduce the vulnerability of stored ammunition, shielding between rounds has been used to prevent initiation of detonation in a round (the acceptor) when one of its neighbors (the donor) detonates. The shielding serves to prevent direct impact of the donor casing or its fragments on the acceptor as well as to process the shock wave entering the acceptor, thus reducing the initiation stimulus. The latter mechanism is amenable to analysis using a hydrodynamic computer code and we have already simulated round to round detonation propagation, with and without shielding, using the 2DE code.[1,2] Shielding effectiveness in reducing shock initiation stimulus levels is further amenable to analysis in one dimension. The present report, therefore, concerns our one-dimensional study of shielding effectiveness using the STEALTH code.[3]

II. SIMULATION DESCRIPTION

The problem elements are the donor, the shield and the acceptor. The acceptor, in the one-dimensional simulation, consists of a steel layer (cover plate or acceptor casing) covering a layer of "inert" TNT. The shield configuration is varied. It consists of a single layer of any of various materials or multiple layers of two different materials. The donor is represented by a layer of steel (flyer plate or donor casing) with an initial velocity on the order of that achieved by the casing of a detonating round. The flyer and cover plate thicknesses are always equal. The problem geometry is illustrated in Figure 1. The "inert" TNT is described by Lee's unreacted JWL equation of state[4] and all other materials by Wilken's LLNL model[3] with 304 steel used for the flyer and cover plates.

---

[1] P.M. Howe, Y.K. Huang and A.L. Arbuckle, "A Numerical Study of Detonation Propagation Between Munitions," Seventh Symposium (International) on Detonation, pp. 1055-1061, June 1981.

[2] J. Starkenberg, Y.K. Huang and A.L. Arbuckle, "A Two-Dimensional Numerical Study of Detonation Propagation Between Munitions by Means of Shock Initiation," BRL Technical Report ARBRL-TR-02522, September 1983.

[3] STEALTH-A Lagrange Explicit Finite Difference Code for Solids, Structural, and Thermohydraulic Analysis, Electric Power Research Institute, November 1981.

[4] E.L. Lee and C.M. Tarver, "Phenomenological Model of Shock Initiation in Heterogeneous Explosives," Physics of Fluids, Volume 23, Number 12, pp. 2362-2372, December 1980.

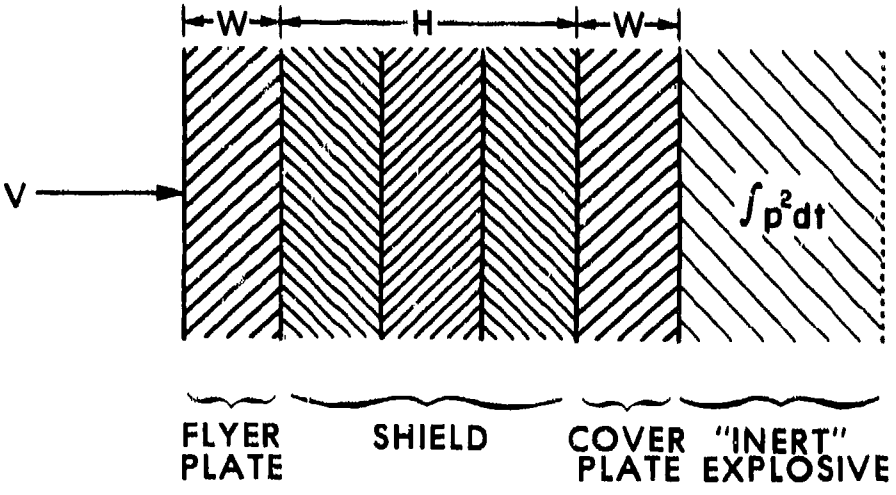

Figure 1. One-Dimensional Representation.

III. CHARACTERIZATION OF THE SHOCK INITIATION STIMULUS

The simplest characterization of shock initiation stimulus levels is the square of the pressure integrated with respect to time ($\int p^2 dt$) evaluated in the acceptor explosive. The use of this integral is an extension of the critical energy concept which is applicable to singly shocked explosives in planar experiments. We have, in general, used this parameter to characterize our computed results. However, the shields often alter the rise time of a single compression wave or produce multiple shock loading in the acceptor. In these cases, the ramp wave or shock waves after the first are not presumed to contribute as significantly as a single shock to the initiation. Thus, integrating through the ramp or including all shocks in the $\int p^2 dt$ calculation produces a conservative estimate of the stimulus (i.e. the actual conditions are even more predisposed toward preventing acceptor initiation). It is also instructive to consider in detail the processing of the shock wave produced by the shield.

IV. RESPONSE OF UNSHIELDED ACCEPTORS

In order to provide baseline data from which to evaluate the stimulus reduction provided by shielding, we ran a number of computations without shielding. This type of loading always produces a single shock in the acceptor as illustrated in Figure 2. In these we varied the casing thickness and impact velocity so as to produce sets of results for constant velocity, constant momentum and constant energy impact. Casing thickness was varied from 5 to 20 mm with appropriate velocities. The results are summarized in Table 1 and plotted in Figure 3. Not surprisingly, as the casing thickness is increased at constant velocity, the initiation stimulus increases rapidly. For constant momentum impacts the stimulus decreases rapidly with increasing casing thickness. Constant energy impacts do not produce a constant stimulus, rather the initiation stimulus decreases slowly with increasing casing thickness. The results of these computations suggest a correlation with $W^{3/5}V^2$, as illustrated in Figure 4.

Table 1. Initiation Stimulus With Unshielded Acceptors

	CONSTANT VELOCITY		CONSTANT MOMENTUM		CONSTANT ENERGY	
CASING THICKNESS W (mm)	VELOCITY V (km/s)	$\int p^2 dt$ (GPa^2-ms)	VELOCITY V (km/s)	$\int p^2 dt$ GPa^2-ms)	VELOCITY V (km/s)	$\int p^2 dt$ (GPa^2-ms)
5.0	1.00	0.074	-	-	1.41	0.170
7.5	1.00	0.112	1.33	0.222	1.15	0.157
10.0	1.00	0.145	1.00	0.145	1.00	0.145
12.5	1.00	0.171	0.80	0.100	0.89	0.129
15.0	1.00	0.190	0.67	0.074	0.82	0.119
17.5	1.00	0.208	0.57	0.054	0.76	0.108
20.0	1.00	0.222	0.50	0.042	0.71	0.098

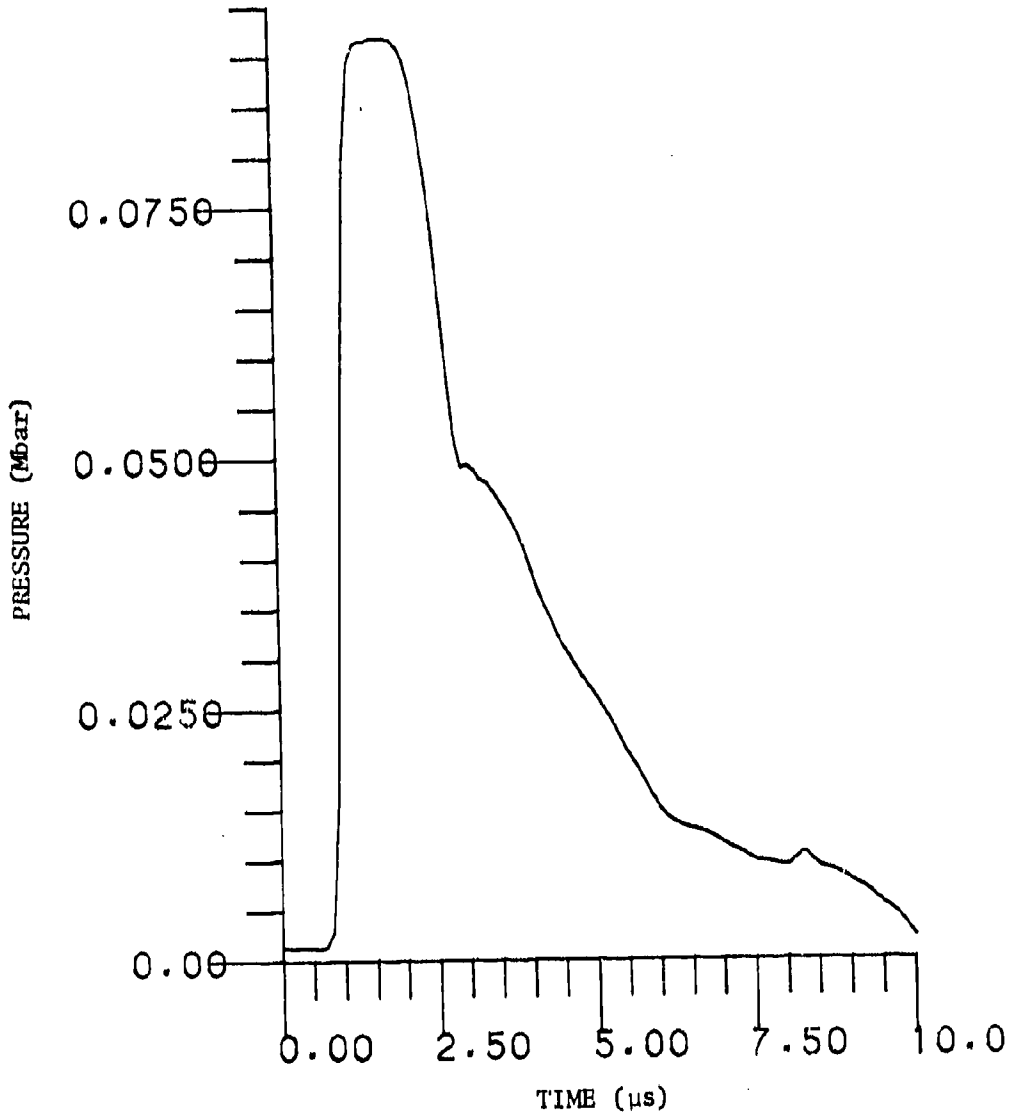

Figure 2. Typical Acceptor Explosive Shock Pressure History without Shielding

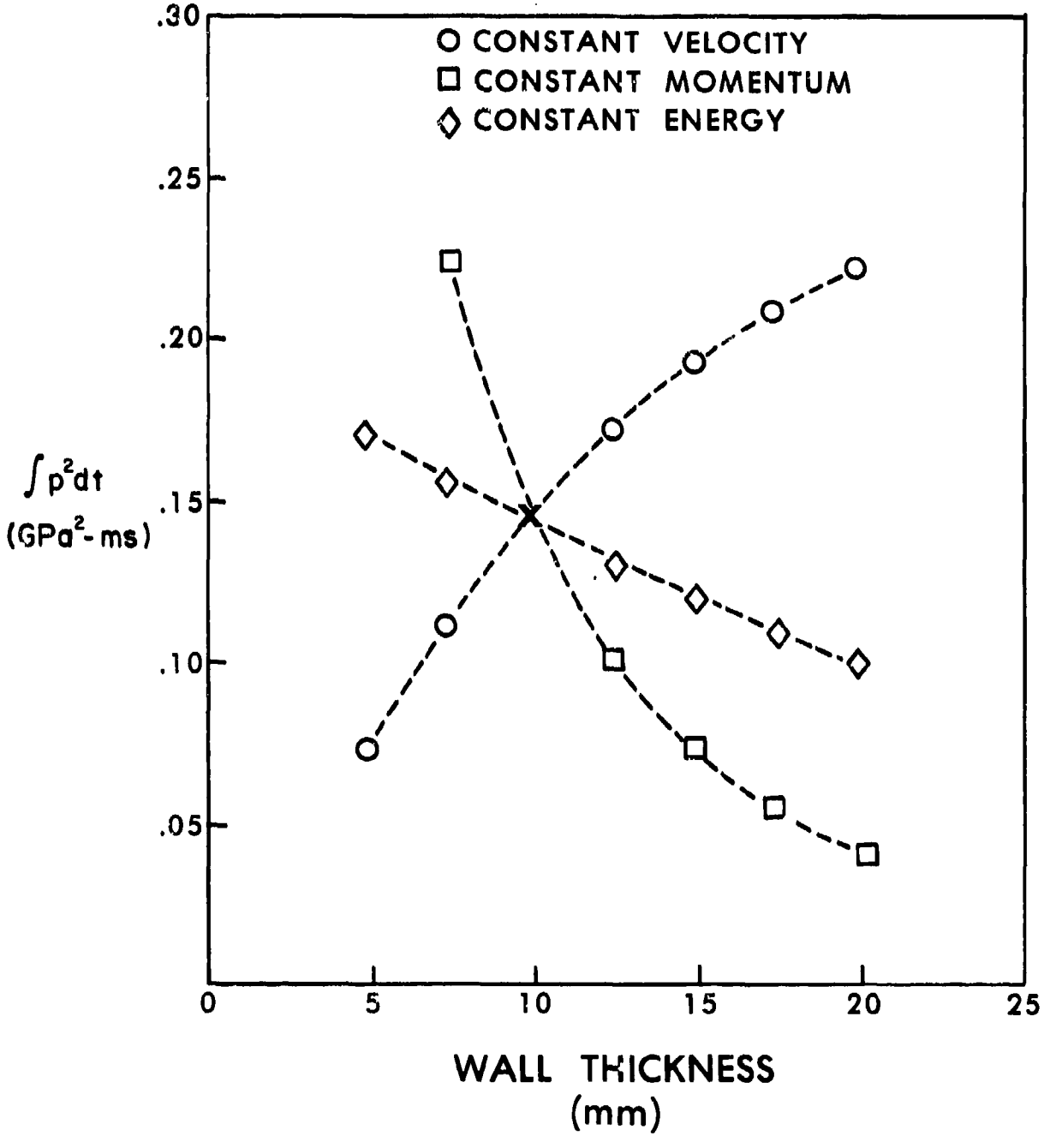

Figure 3. Variation of Shock Initiation Stimulus with Wall Thickness in the Absence of Shielding

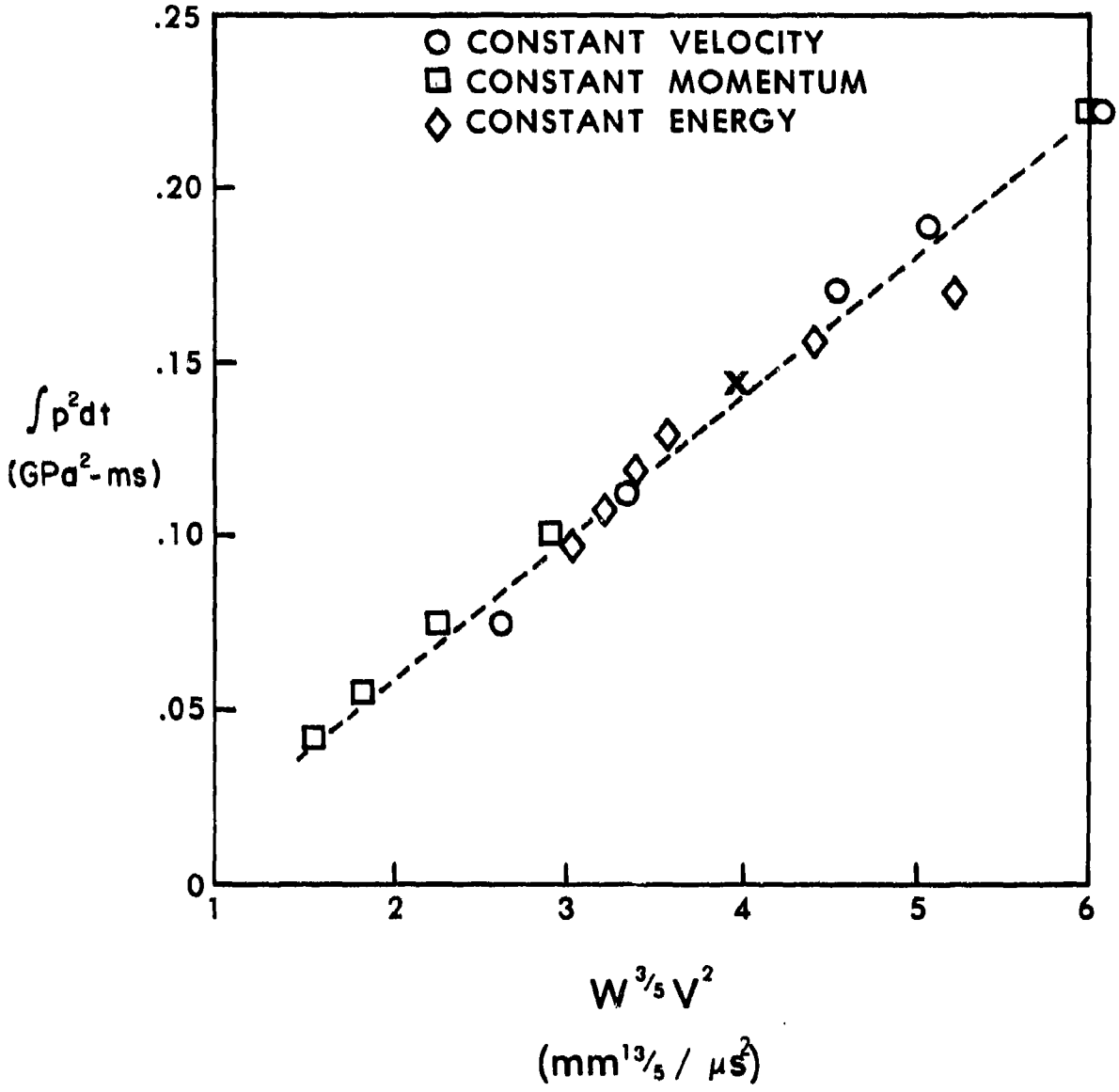

Figure 4. Correlation of Shock Initiation Stimulus with Flyer and Cover Plate Parameters.

V. RESULTS WITH SINGLE LAYERED SHIELDS

A. General

Our version of the STEALTH code is accompanied by a materials library providing standard preprogrammed material models. The vast majority of these are for metallic elements and alloys. The only plastic material description available is for Lucite. Nonetheless, we made computations with 10 mm thick casings and various shield thicknesses for each available material. Special emphasis was given to Lucite, tungsten and steel. The impact velocity was held at 1 km/s.

B. Shock Structure

The pressure history in the acceptor explosive depends on the casing thickness, the shield thickness and the shock impedance of the shield. When the impedance of the shield is lower than that of the casing, a shock wave reverberates between the donor and acceptor casings, delivering repeated shocks to the acceptor. Our lowest impedance material is Lucite. Figure 5 illustrates this effect for 5, 15, 25 and 35 mm thick Lucite shields. Clear separation of three shocks of increasing amplitude may be observed in Figure 5c for a 25 mm thick shield. The complete pulse is about 14 μs long with a peak pressure of 35 GPa (.035 Mbar). For the 15 mm thick shield of Figure 5b, the first shock is clearly defined while the second shock appears intermingled with the third. This pulse is about 12 μs in duration with a 4.2 GPa (.042 Mbar) peak. With a 5 mm thick shield, all the shocks have coalesced into a 10 ms pulse with a 5.1 GPa (.051 Mbar) peak, as illustrated in Figure 5a. Thus the effect of increasing shield thickness is to increase the interval between shocks, lengthen the pulse duration and reduce the peak pressure. The temporal spacing between the shock fronts generated at the shield/acceptor casing interface depends on shield thickness since two shock transits across the shield occur between the generating interactions. As these shocks propagate into the acceptor, they tend to coalesce so that, if the initial temporal spacing is small enough, the shocks will not be distinguishable from one another when they arrive at the acceptor explosive. Because of this coalescence, shock breakup was only observed for Lucite and magnesium (see Figure 6).

When the impedance of the shield is higher than that of the casing a single shock in the acceptor is always observed. Our highest impedance material is tungsten. Figure 7 shows the shocks produced with 5, 15, 25 and 35 mm thick tungsten shields. The effect of increasing shield thickness is to slightly increase pulse duration while substantially reducing peak pressure.

C. Initiation Stimulus Reduction

The effect of shield material on shock initiation stimulus reduction as measured by $\int p^2 dt$ is illustrated in Figure 8. This is a plot of $\int p^2 dt$ versus initial acoustic impedance for 30 mm thick shields. The results are segregated into two groups. One group includes most of the materials whose initial acoustic impedance is less than that of steel and the other group is comprised primarily of materials whose initial acoustic impedance is greater than that of steel. Exceptions are that nickel with a slightly greater

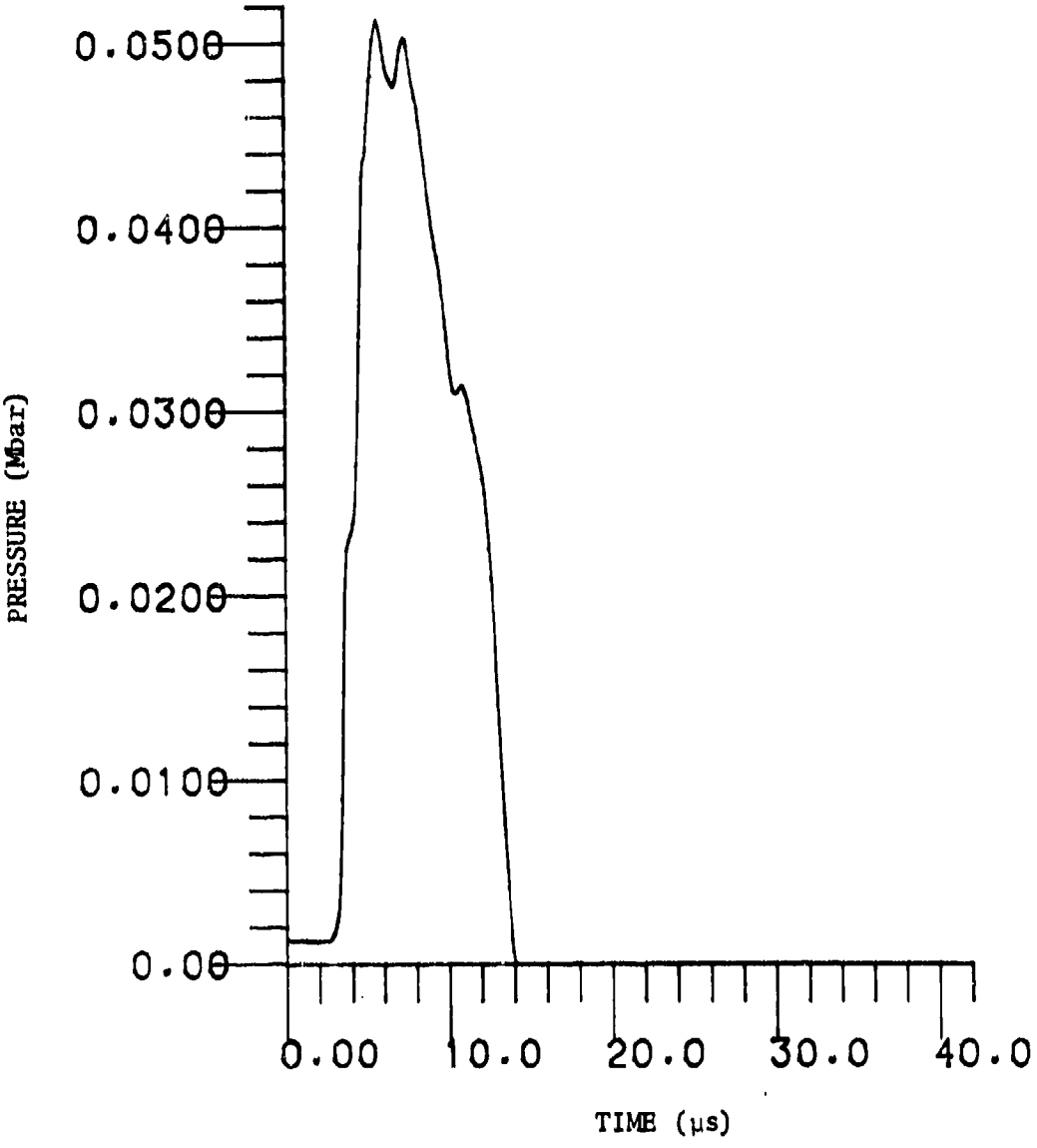

Figure 5a. Acceptor Explosive Pressure History with 5-mm Thick Lucite Shield

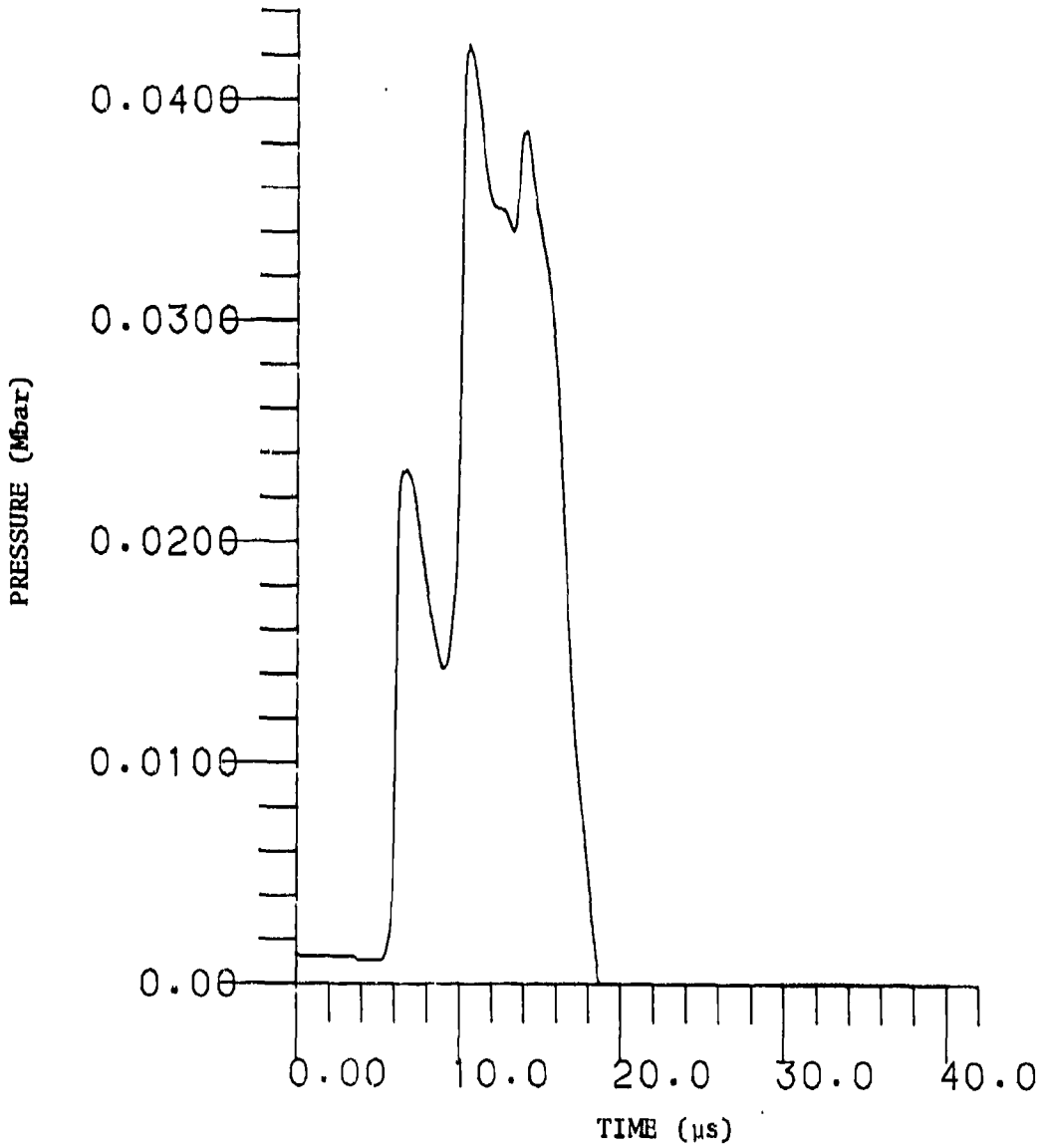

Figure 5b. Acceptor Explosive Pressure History with 15-mm Thick Lucite Shield

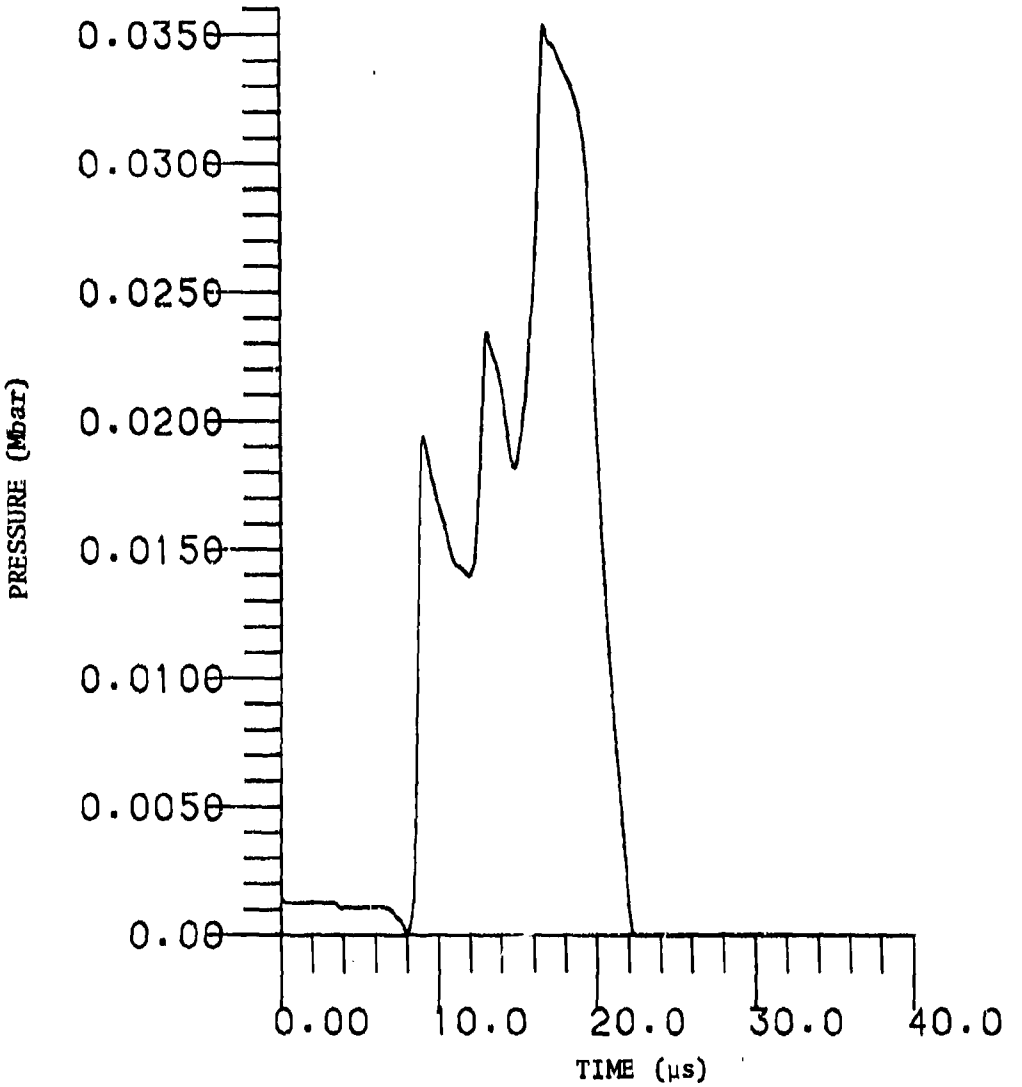

Figure 5a. Acceptor Explosive Pressure History with 25-mm Thick Lucite Shield

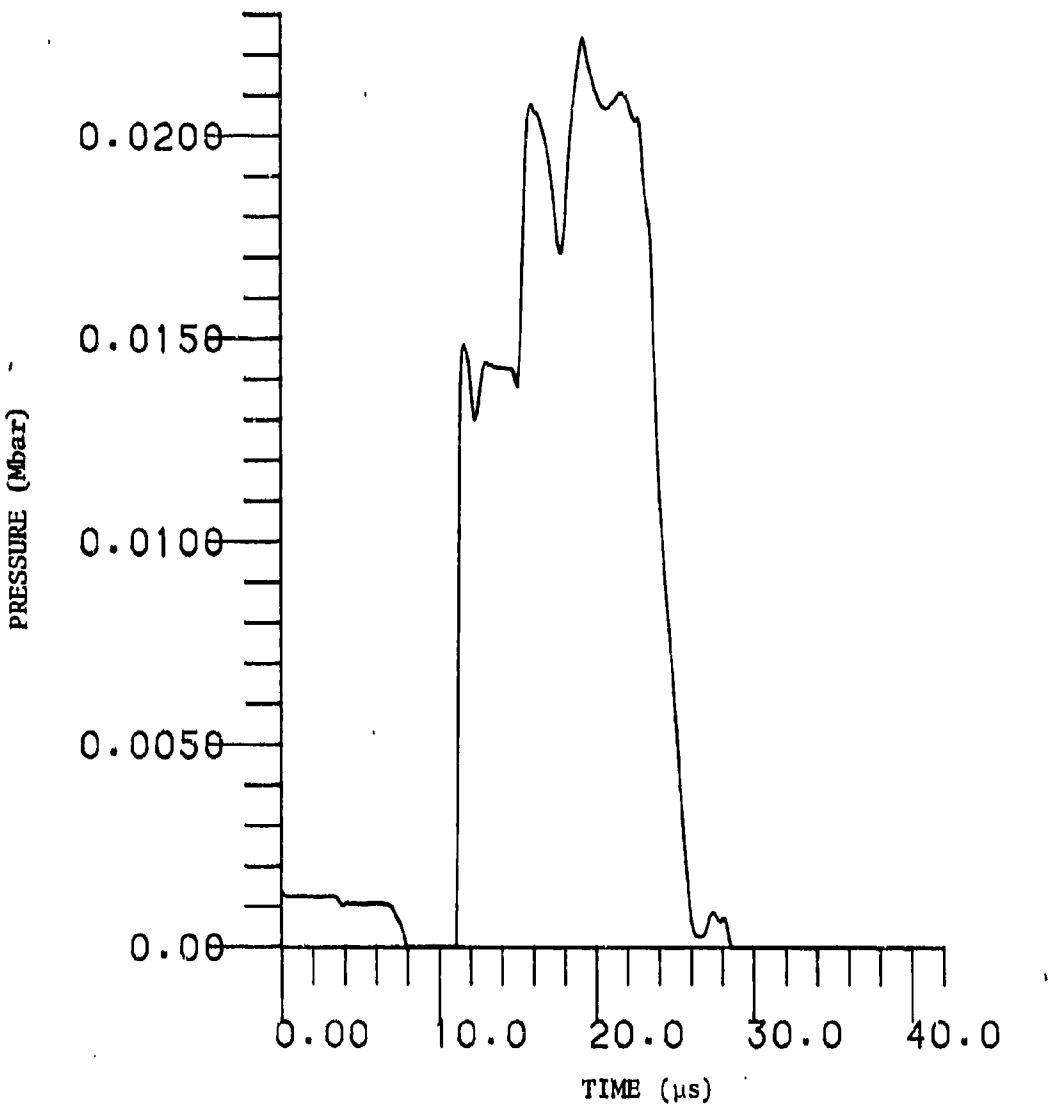

Figure 5d. Acceptor Explosive Pressure History with 35-mm Thick Lucite Shield

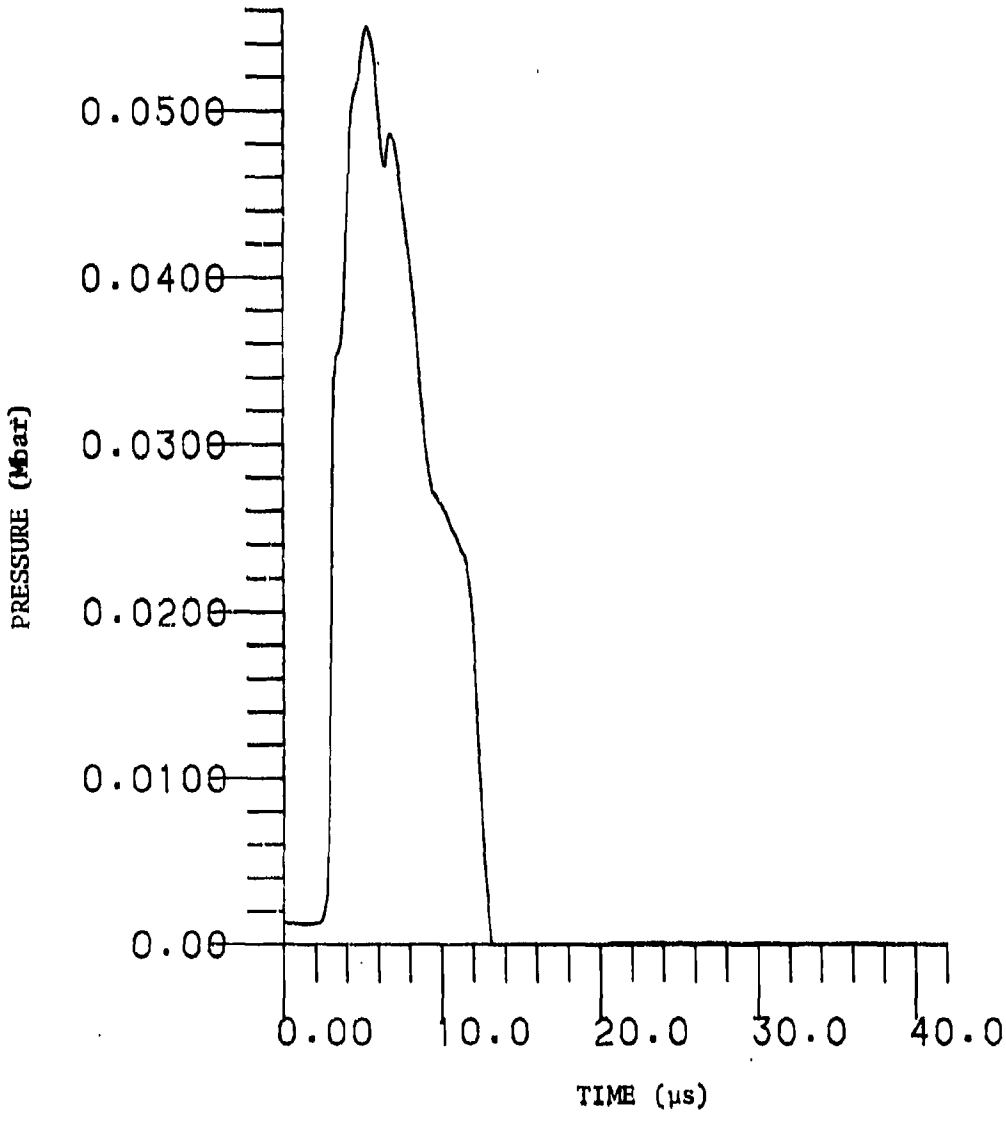

Figure 6a. Acceptor Explosive Pressure History with 5-mm Thick Magnesium Shield

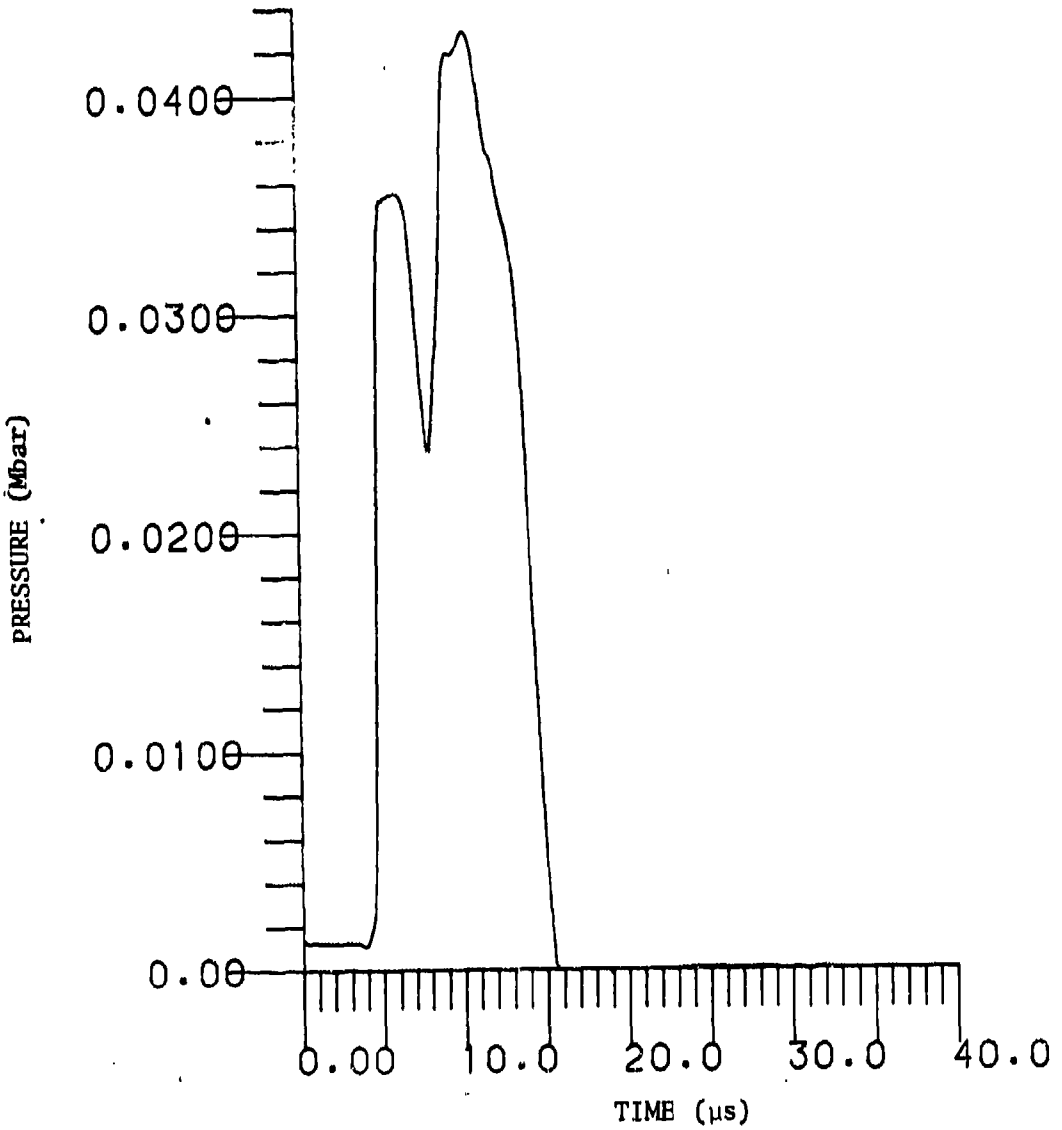

Figure 6b. Acceptor Explosive Pressure History with 15-mm Thick Magnesium Shield

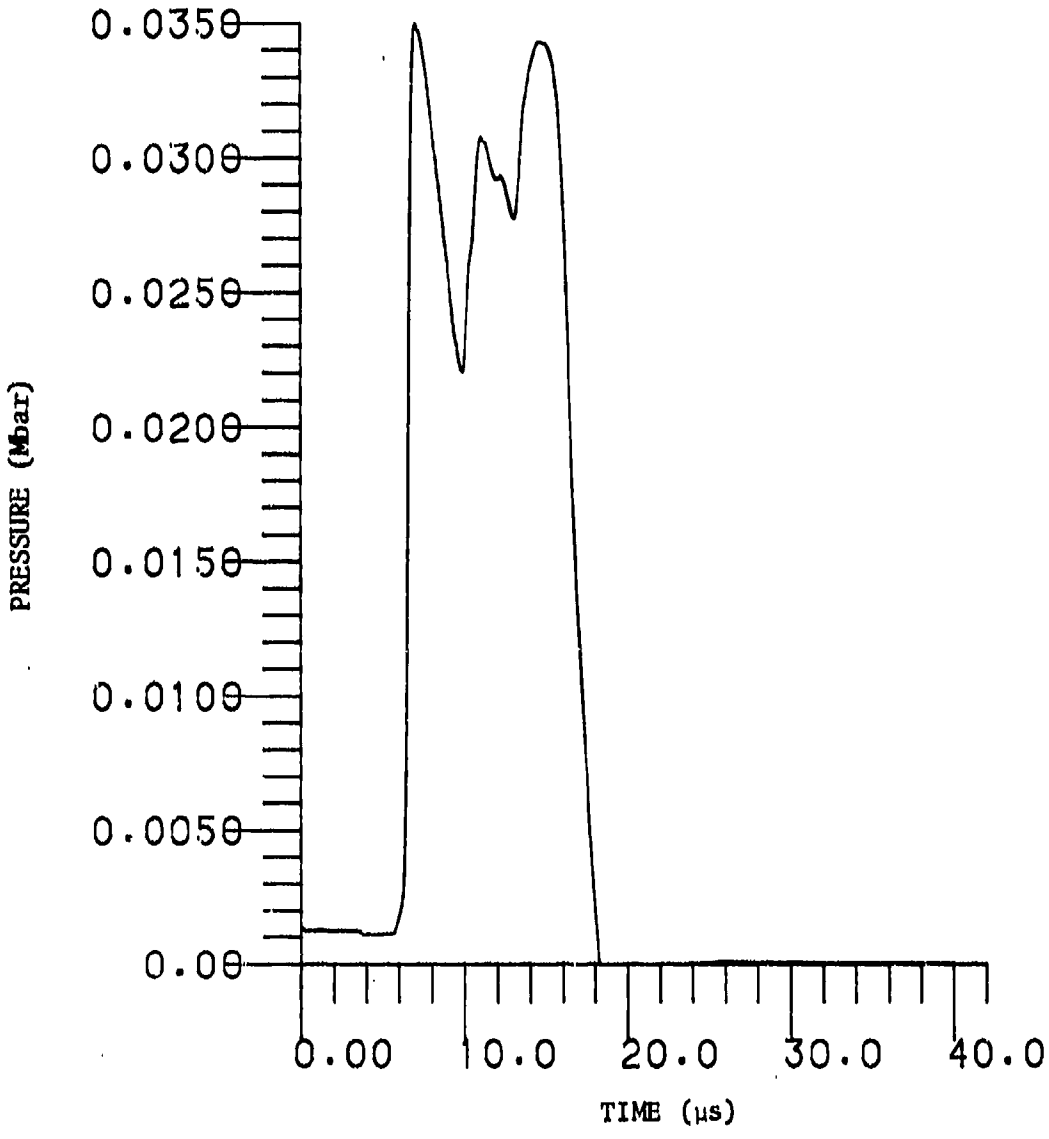

Figure 6a. Acceptor Explosive Pressure History with 25-mm Thick Magnesium Shield

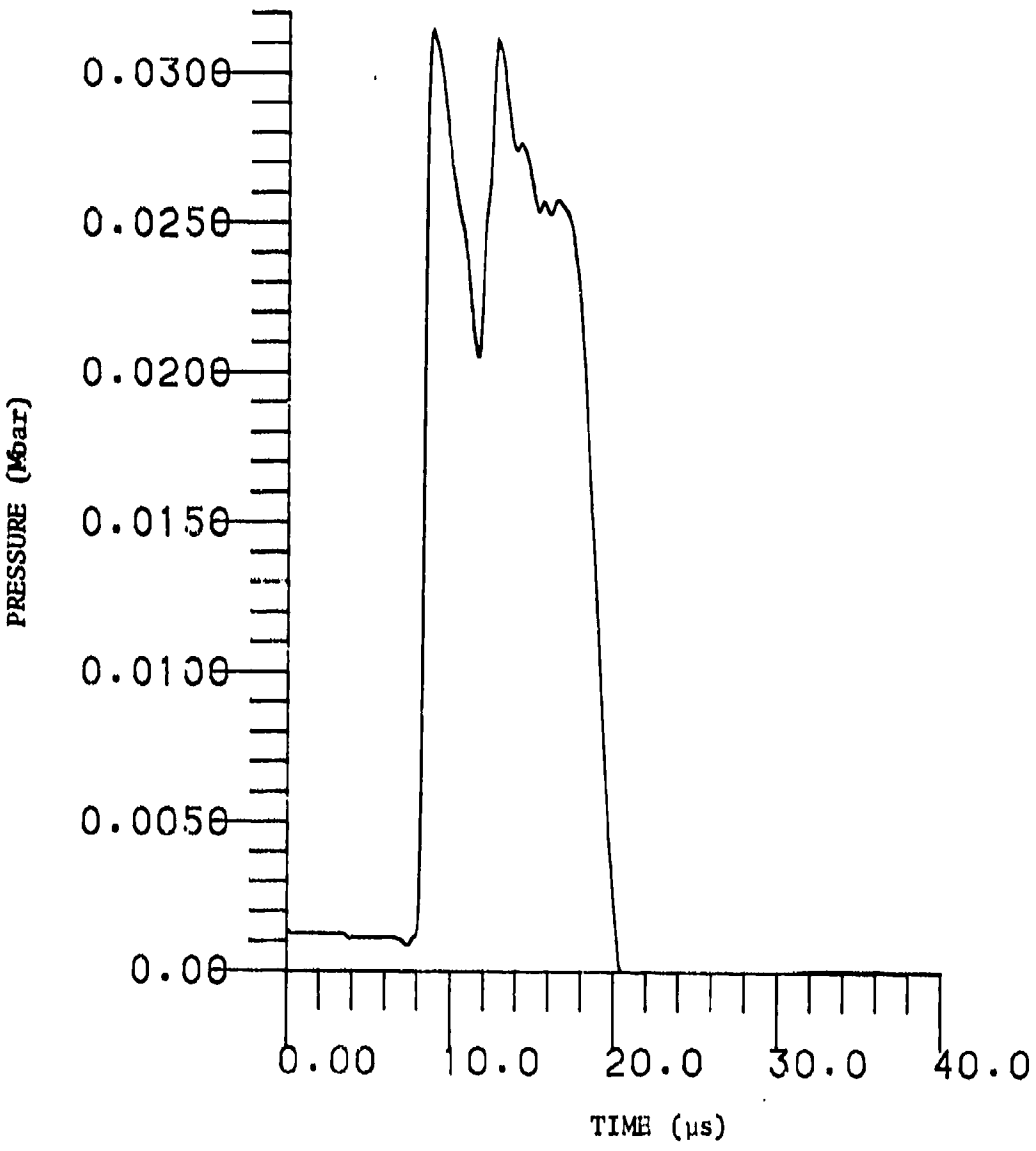

Figure 6d. Acceptor Explosive Pressure History with 35-mm Thick Magnesium Shield

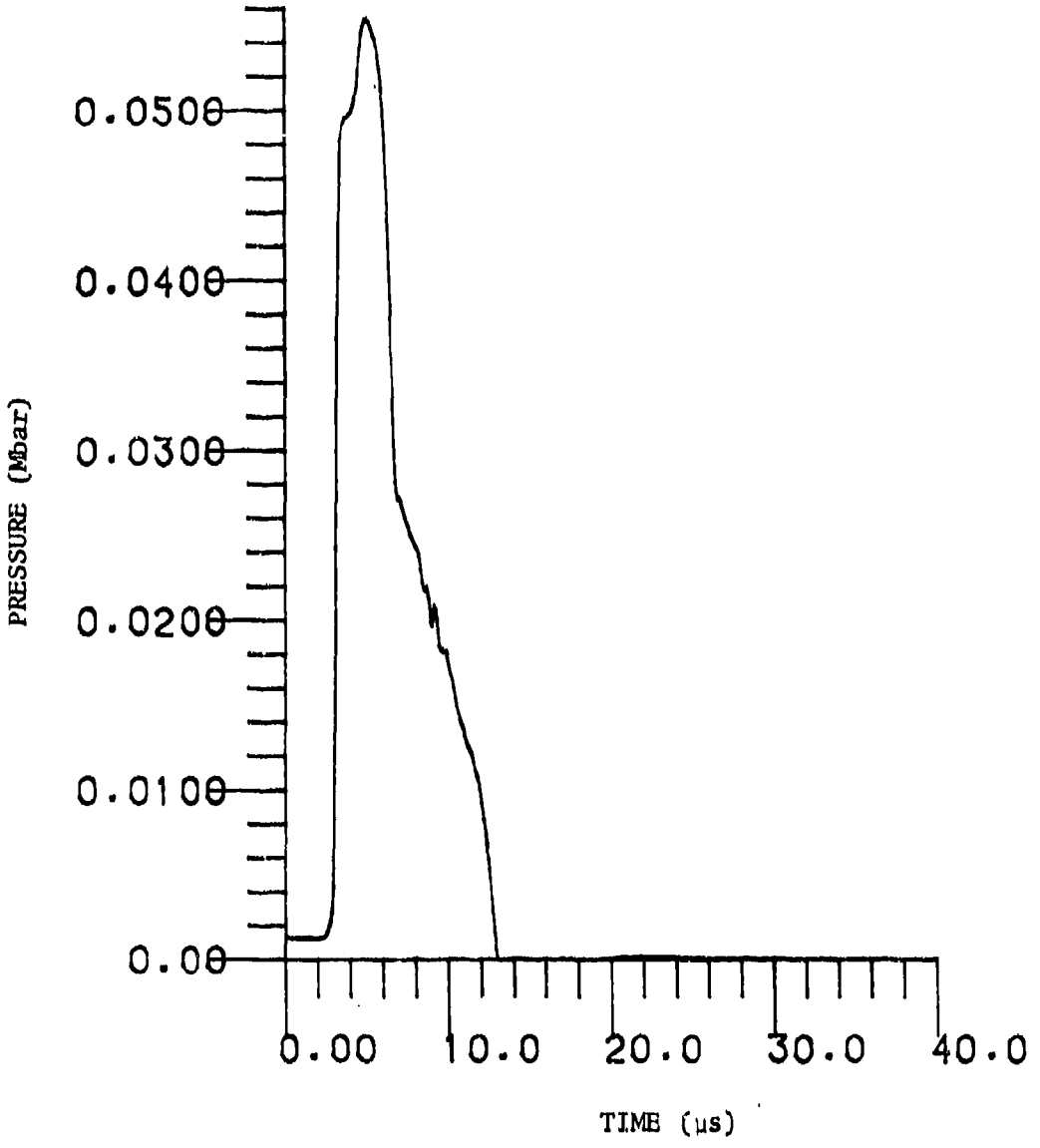

Figure 7a. Acceptor Explosive Pressure History with 5-mm Thick Tungsten Shield

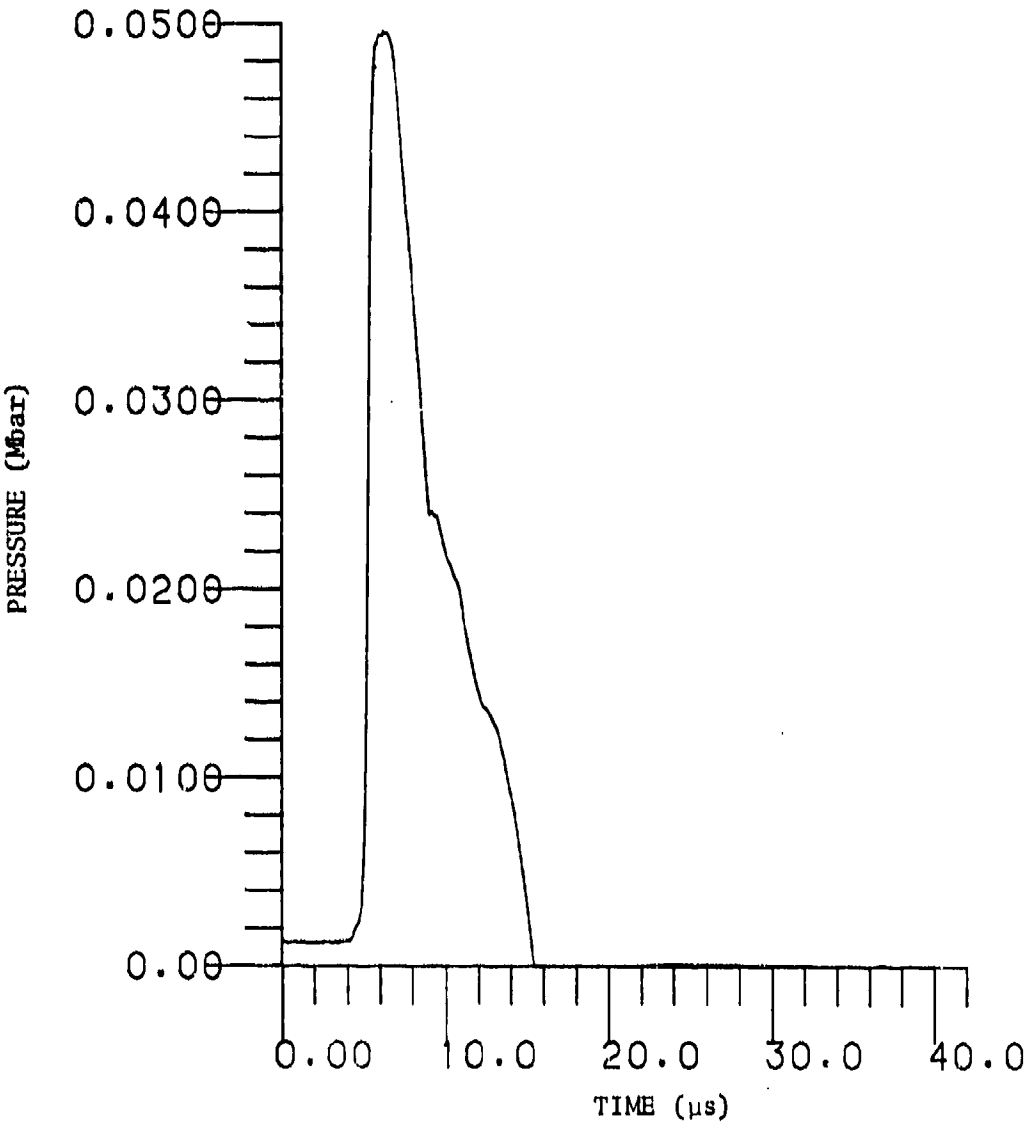

Figure 7b. Acceptor Explosive Pressure History with 15-mm Thick Tungsten Shield

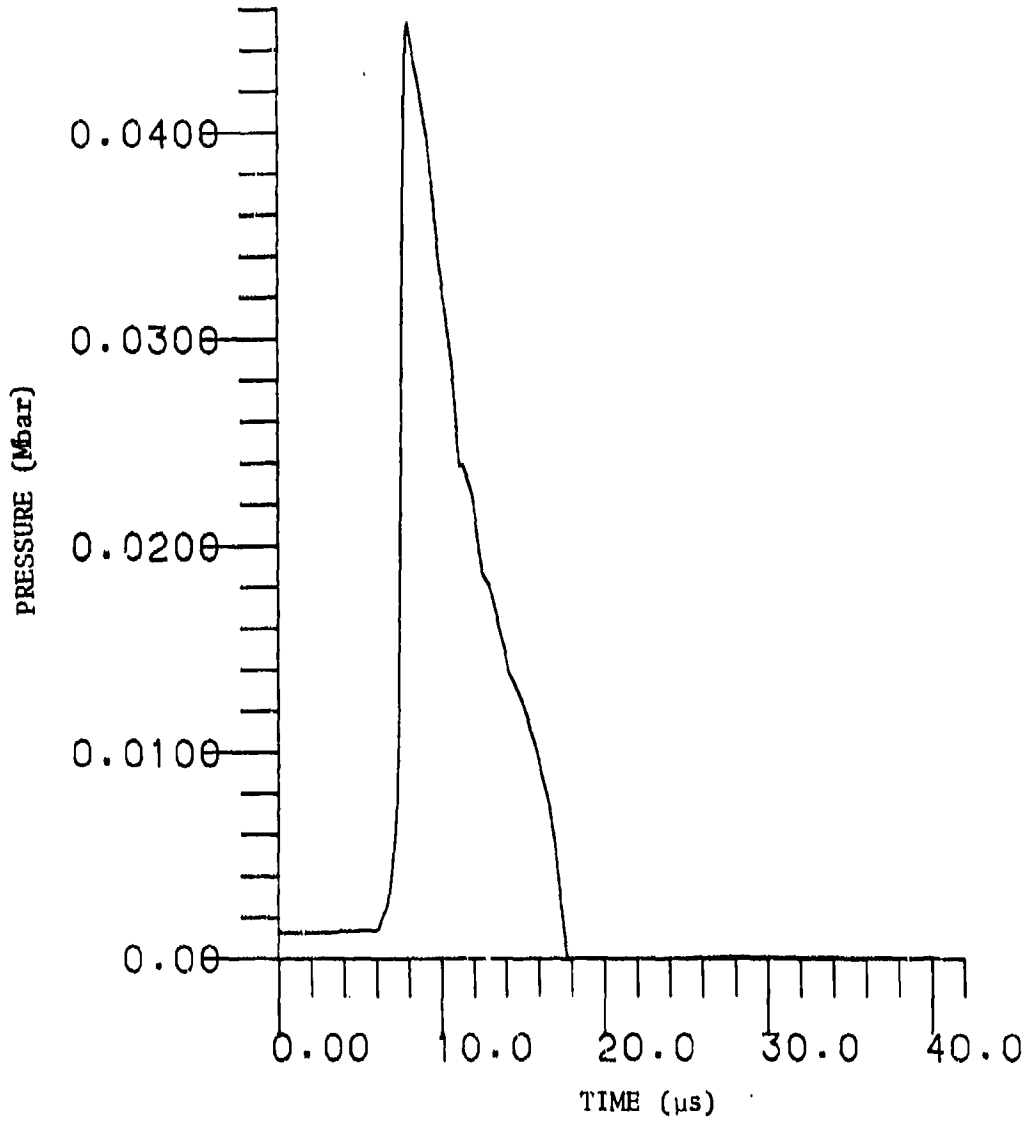

Figure 7a. Acceptor Explosive Pressure History with 25-mm Thick Tungsten Shield

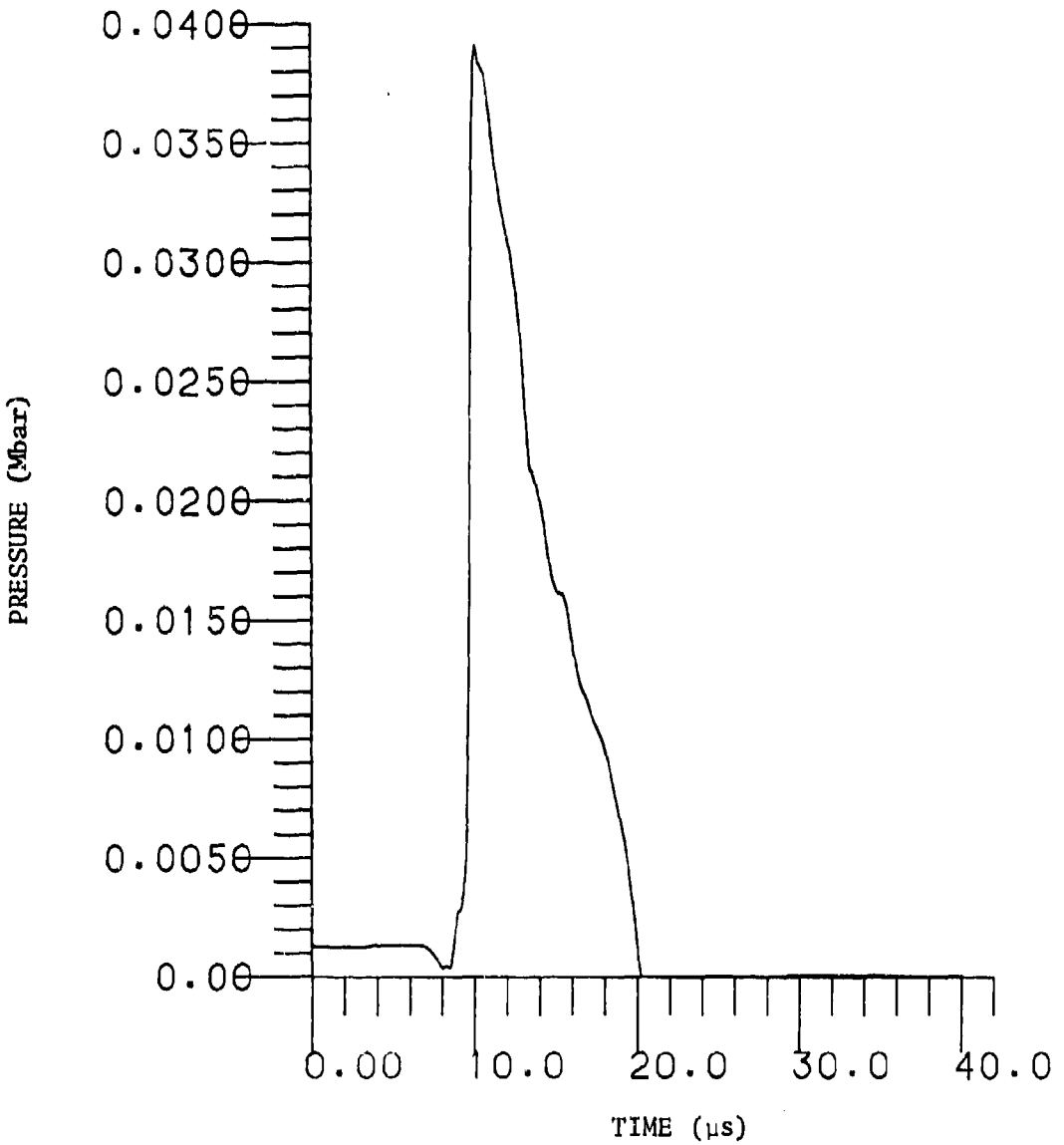

Figure 7d. Acceptor Explosive Pressure History with 35-mm Thick Tungsten Shield

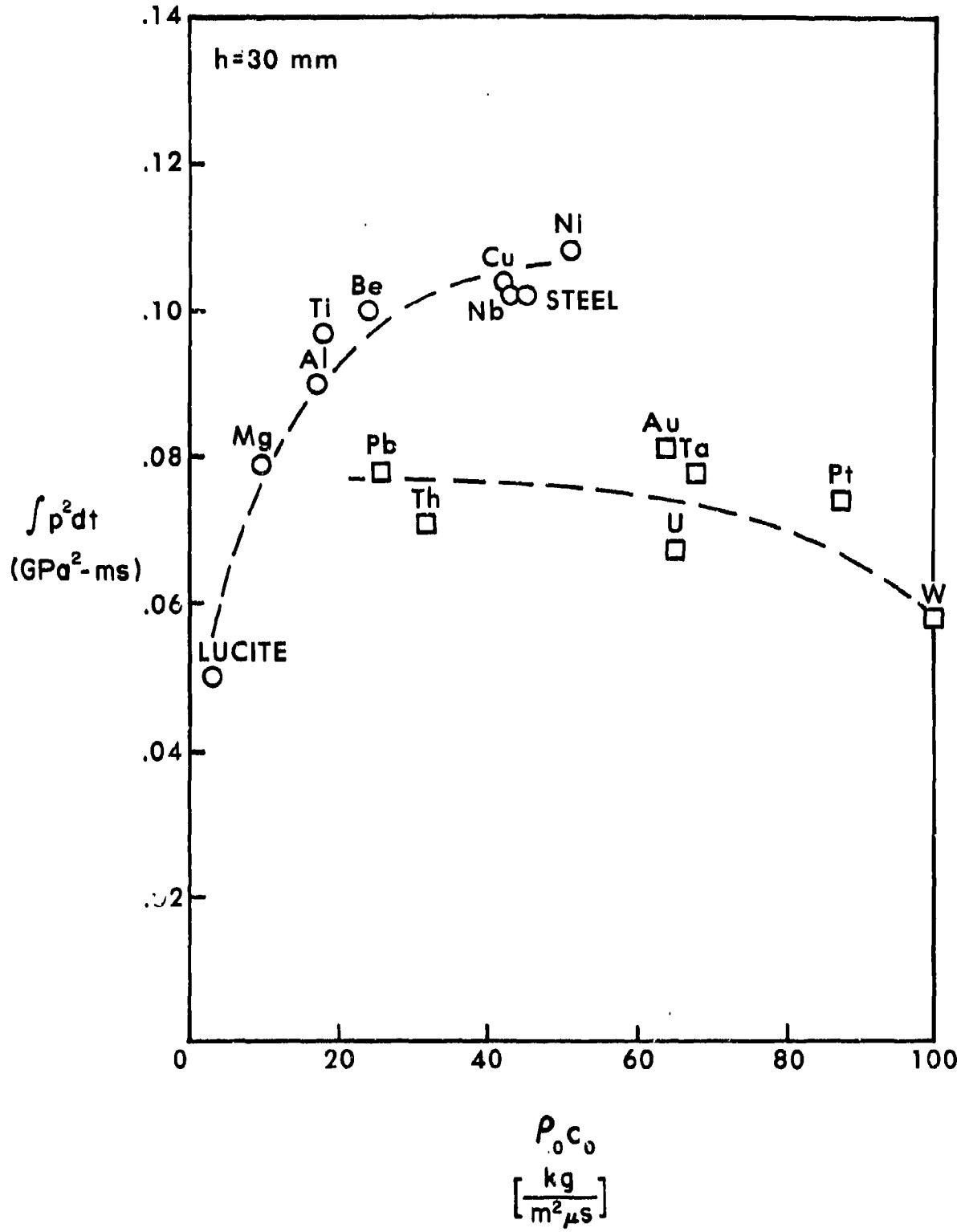

Figure 8. Variation of Shock Initiation Stimulus with Initial Acoustic Impedance of 30-mm Thick Shields

initial impedance than steel belongs to the low impedance group and lead and thorium with lower impedance than steel appear to belong to the higher impedance group (although the latter classification is more questionable). As impedance increases among the low impedance materials, the initiation stimulus approaches that associated with steel shields, which provide the lowest level of protection. Materials in the high impedance group, on the other hand, do not appear to produce stimulus levels approaching that of steel, but they provide greater protection than all but the lowest impedance materials.

The effect of shield thickness is illustrated in Figure 9 which is a plot of $\int p^2 dt$ versus shield thickness for Lucite, steel and tungsten. The results show that steel provides the least protection, except for shields less than about 6 mm thick where Lucite is worst, and tungsten provides the best protection except for shields between about 27 mm and 50 mm thick where Lucite is slightly better. Stimulus reduction increases with shield thickness for all three materials. The increase is most marked for Lucite, which also shows a leveling off for shield thicknesses greater than 40 mm at which point little additional protection is provided with increasing thickness.

VI. RESULTS WITH MULTILAYERED SHIELDS

A. General

Shields with multiple layers provide additional impedance discontinuities which can further reduce the shock initiation stimulus. We have examined the effectiveness of three and five layer shields composed of alternate layers of our lowest and highest impedance materials, Lucite and tungsten, and of alternate layers of Lucite and steel as well. The order of the materials and the relative thickness of the layers was varied but, except in the study of shield thickness, all of the shields were 30 mm thick. Symmetry was always maintained. The impact velocity was held at 1 km/s.

When the total shield thickness is fixed, three-layered shields may be completely specified by the Lucite thickness fraction (i.e. the total thickness of all Lucite layers divided by the shield thickness, h) with five-layered shields, an additional degree of freedom arises since the thickness of the innermost layer need not equal the thickness of the two outer layers of the same material. This degree of freedom is accounted for by the parameter $z=h_1/(h-h_o)$ where h_1 is the thickness of the central layer and h_o the thickness of the outer layers. When z=0, the shield is reduced to three layers; and when $z= h_1/h$, the shield also has three layers but with the material order reversed.

B. Shock Structure

Three-layered shields composed of Lucite and tungsten may have either component in the inner layer. Figure 10 illustrates the pressure history in the acceptor for shields consisting of an inner layer of Lucite surrounded by layers of tungsten. When the shield is composed mostly of tungsten, as in Figure 10a, a single shock enters the acceptor. Figure 10b shows results for a shield with a little more Lucite. Some structure at the tail of the wave

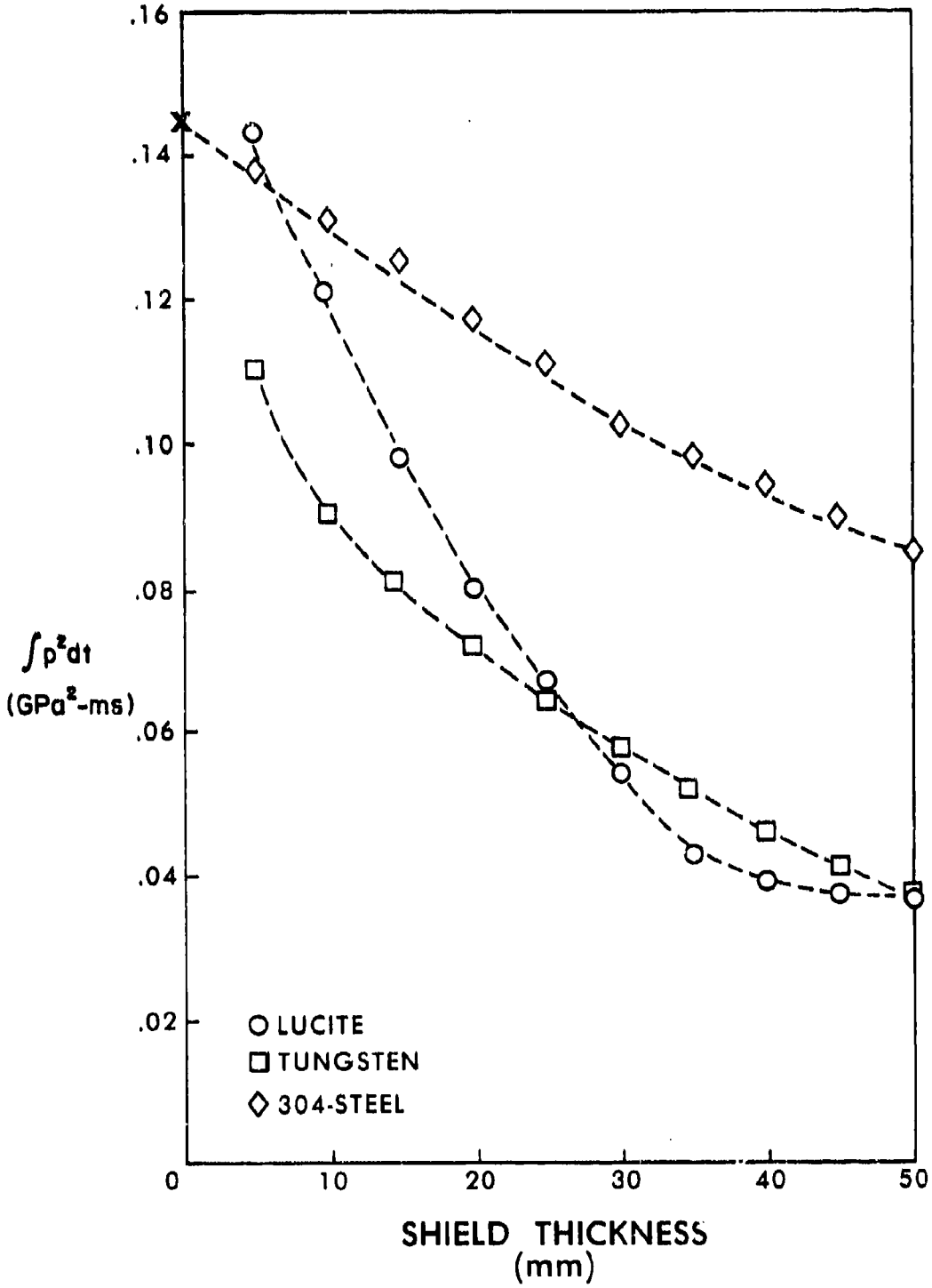

Figure 9. Variation of Shock Initiation Stimulus with Shield Thickness for Lucite, Tungsten and 304-Steel Shields

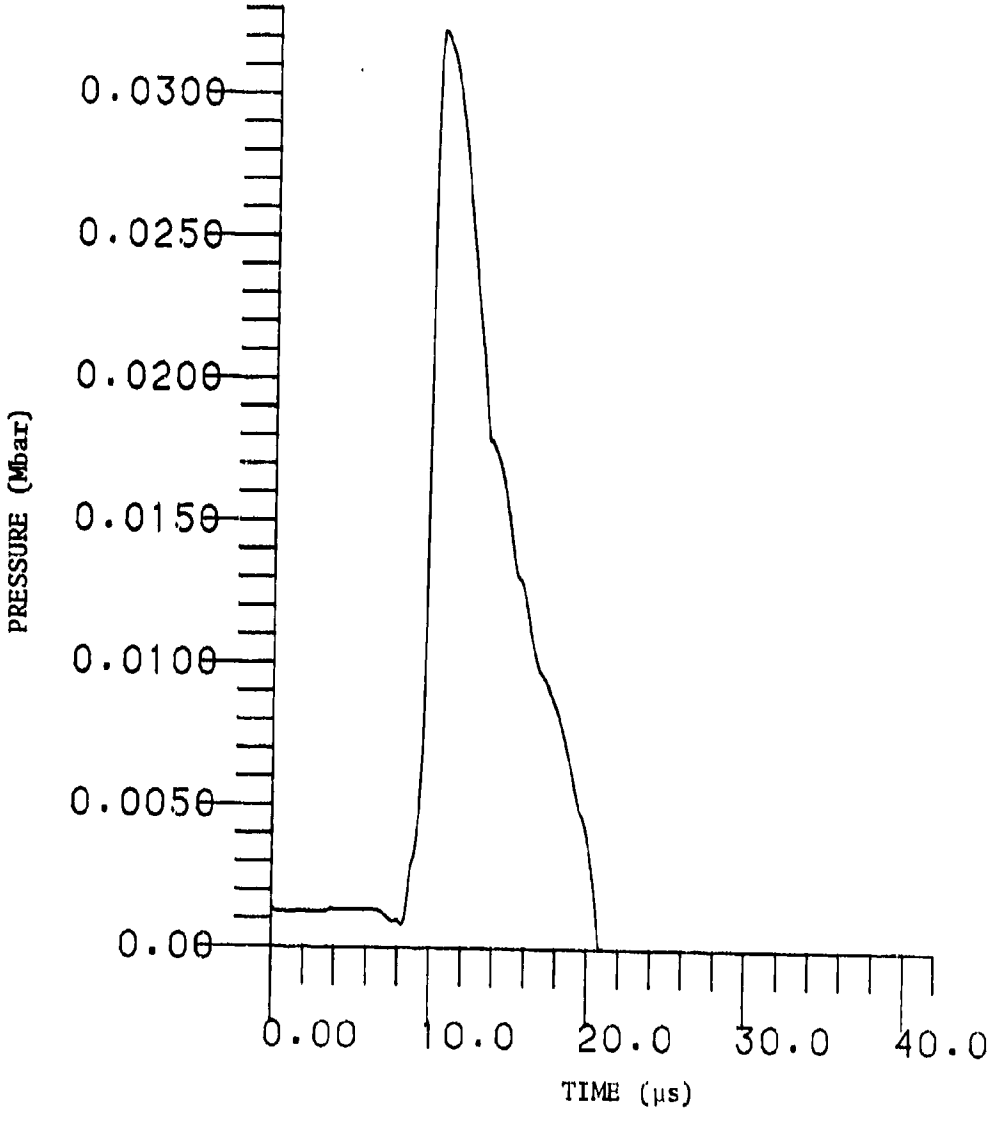

Figure 10a. Acceptor Explosive Pressure History with 30-mm Thick Three-Layered Tungsten/Lucite/Tungsten Shield at 8.3% Lucite

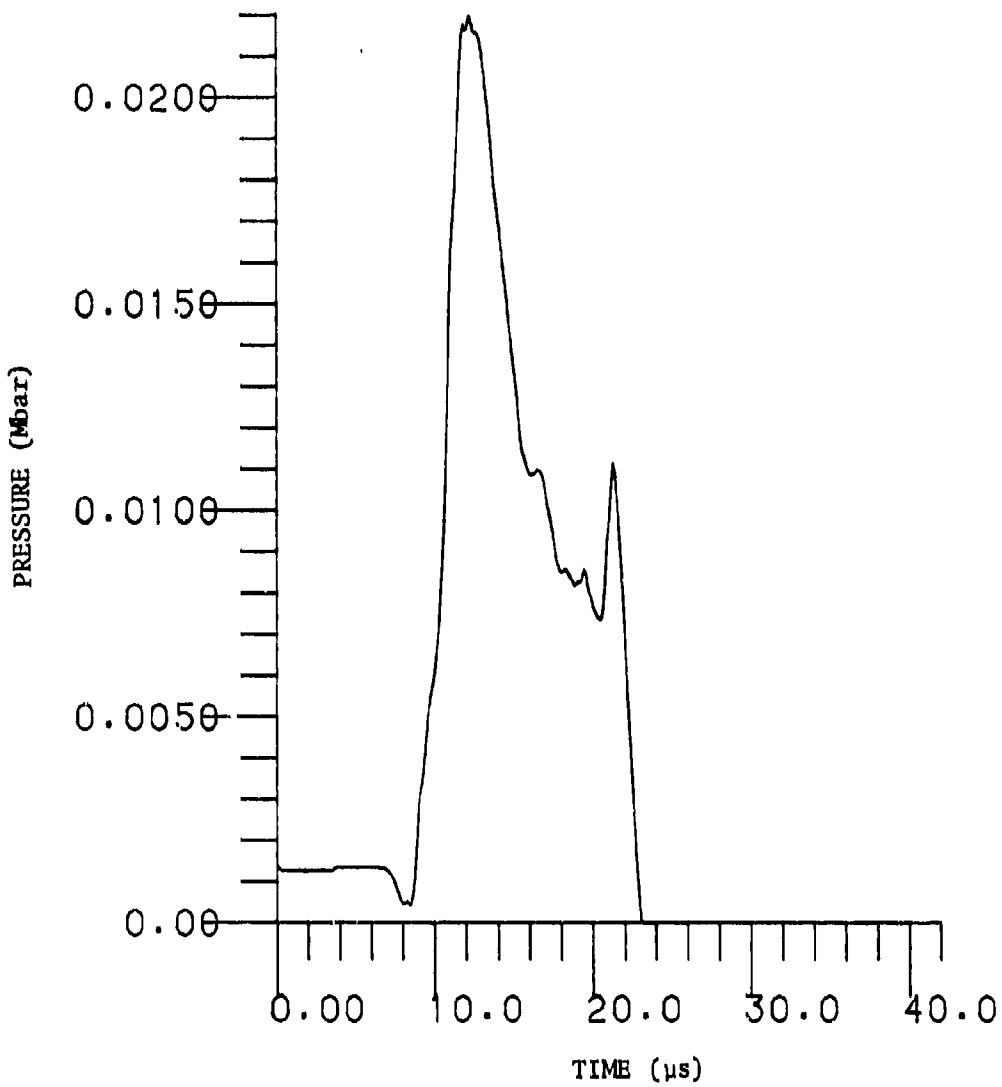

Figure 10b. Acceptor Explosive Pressure History with 30-mm Thick Three-Layered Tungsten/Lucite/Tungsten Shield at 16.7% Lucite

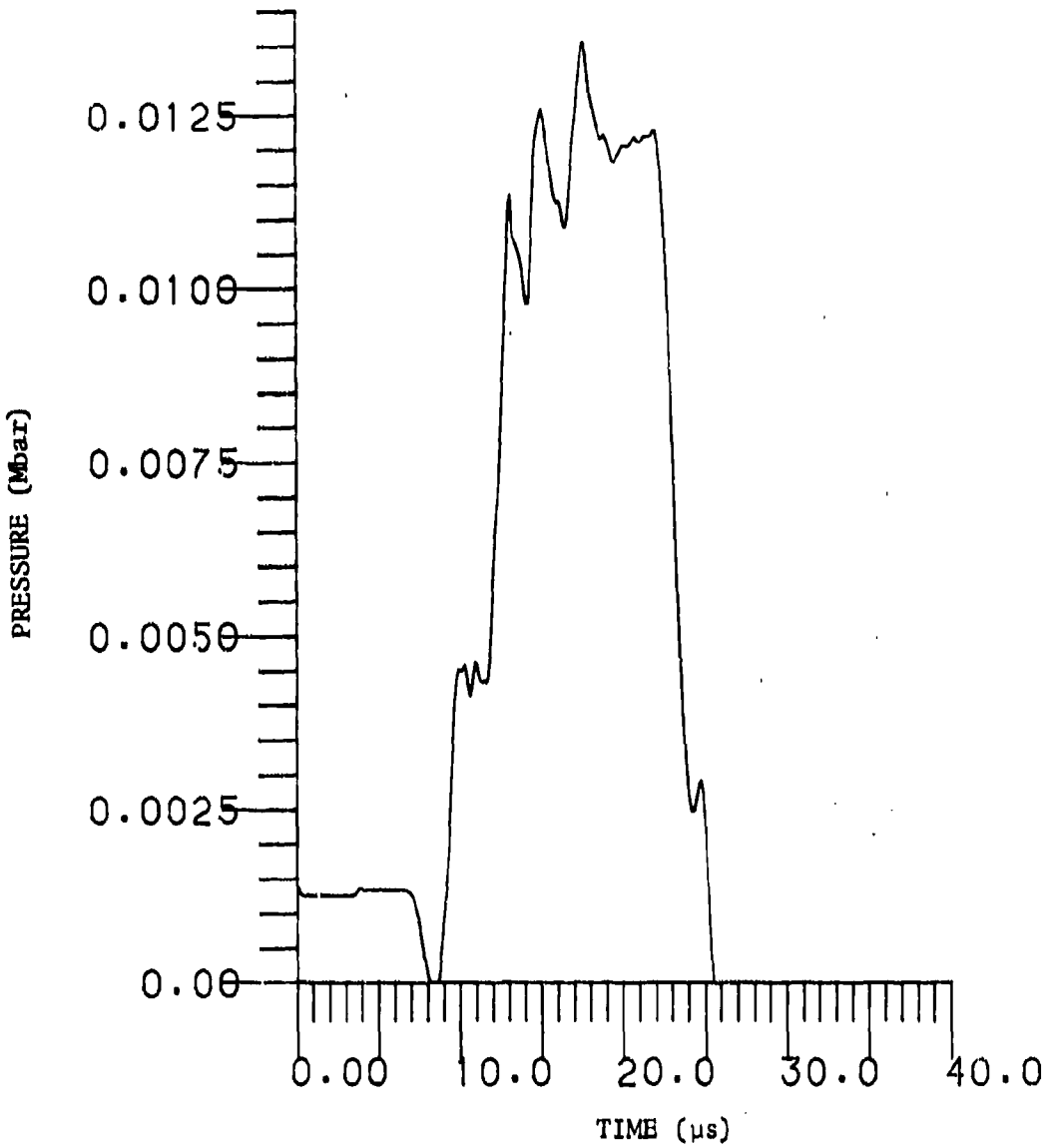

Figure 10c. Acceptor Explosive Pressure History with 30-mm Thick Three-Layered Tungsten/Lucite/Tungsten Shield at 33.3% Lucite

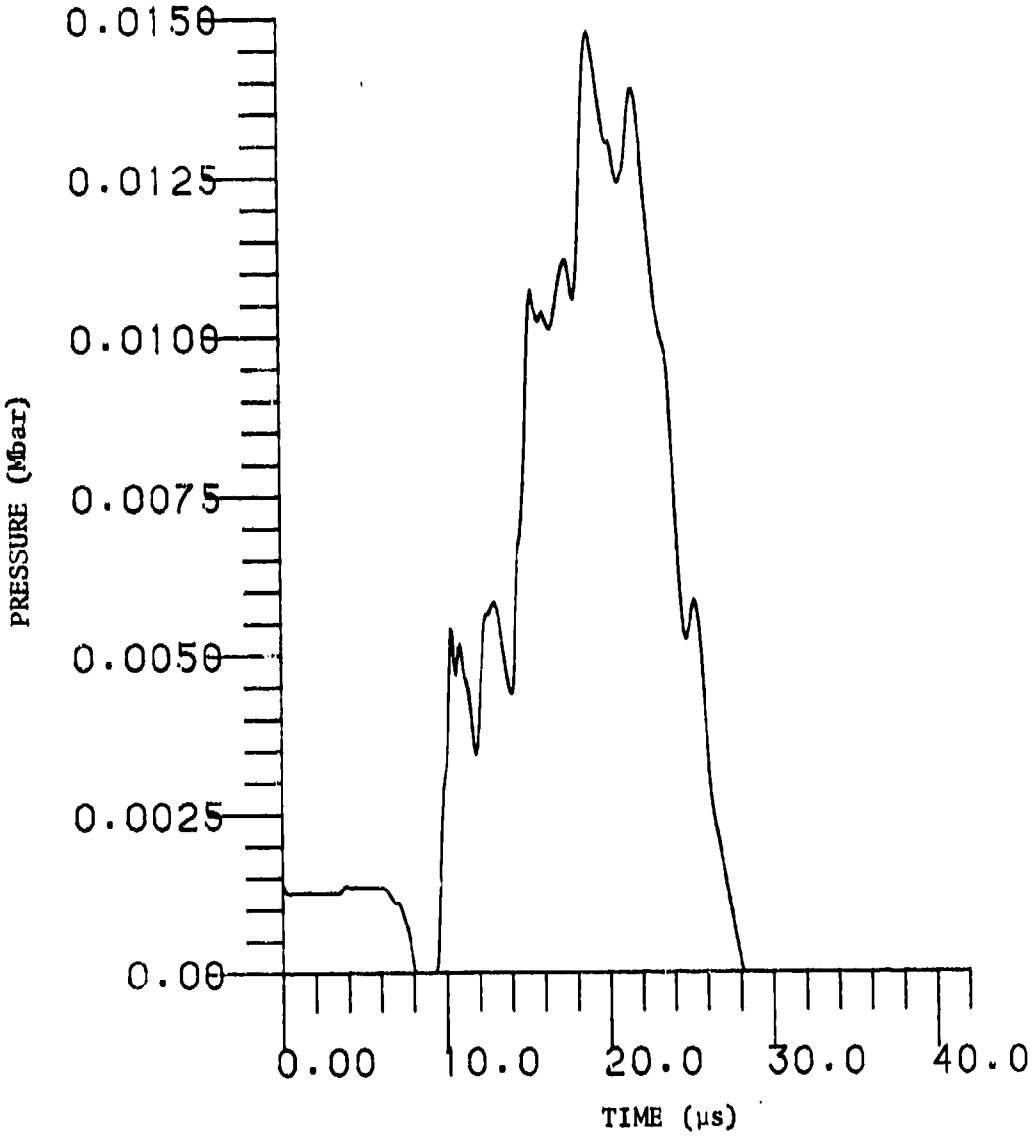

Figure 10d. Acceptor Explosive Pressure History with 30-mm Thick Three-Layered Tungsten/Lucite/Tungsten Shield at 50% Lucite

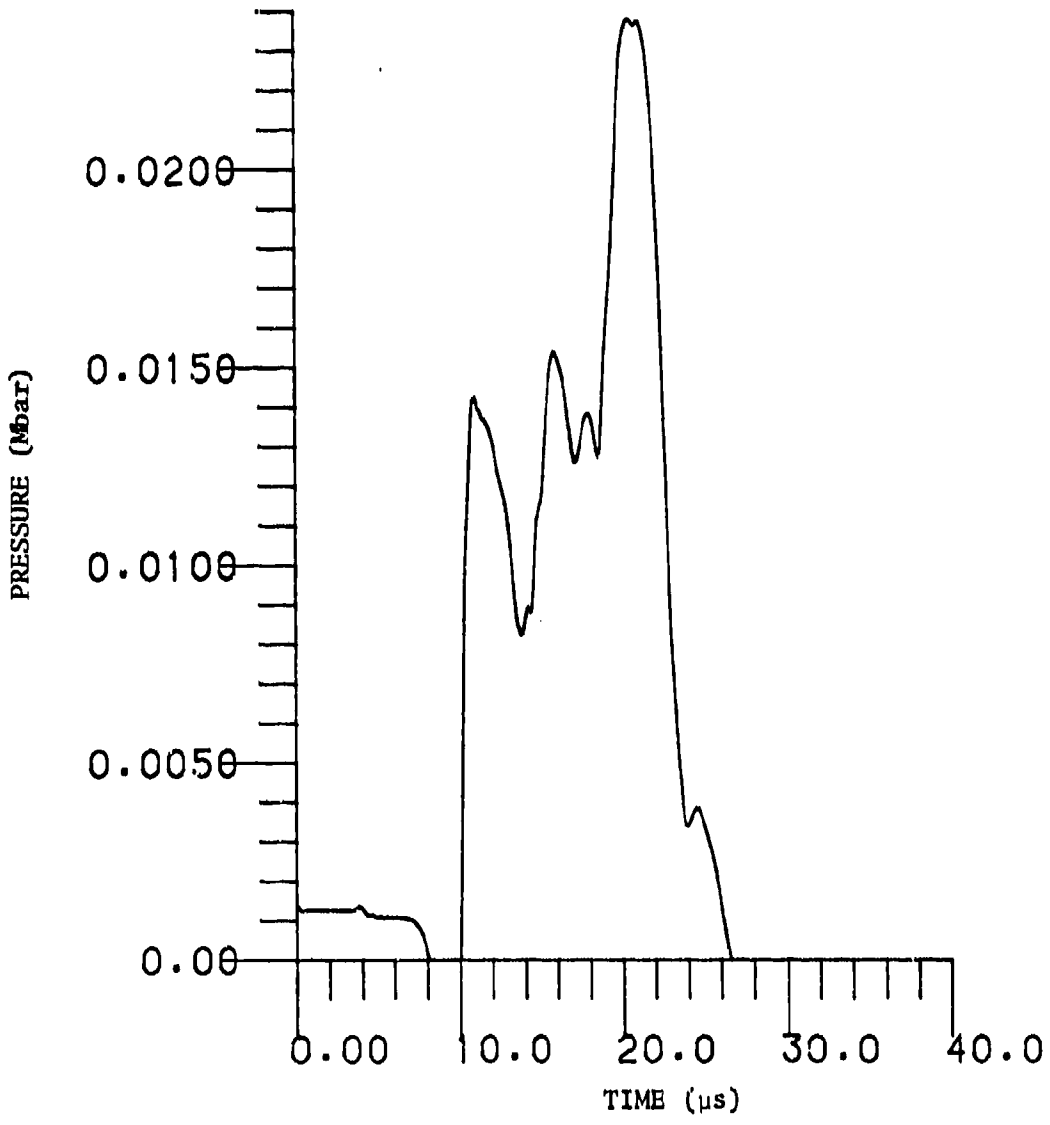

Figure 10e. Acceptor Explosive Pressure History with 30-mm Thick Three-Layered Tungsten/Lucite/Tungsten Shield at 91.7% Lucite

may be noted but this is still primarily a single shock. With a still higher Lucite fraction, the shock structure is altered radically and multiple shock loading is observed as shown in Figure 10c through 10e. The transition to multiple shocks occurs somewhere between 17 and 33 percent Lucite and minimum pressure levels occur at about 33 percent Lucite.

When tungsten is the inner component of the shield, the results are somewhat different as illustrated in Figure 11. In this case a single pulse is usually produced but the peak pressure and rise time of the compression depend upon the Lucite thickness fraction as indicated in Table 2. This shows the pressurization rate to be minimum at about 50 percent Lucite. Multiple shock structure does not appear until the shield is nearly all Lucite as shown in Figure 11d.

Table 2. Compression Wave Characteristics for Lucite/Tungsten/Lucite Shields

Shield Configuration (mm/mm/mm)	Lucite Fraction	Peak Pressure (GPa)	Rise Time (μs)	Pressurization Rate (GPa/μs)
1.25/27.5/1.25	.083	3.95	1.6	2.47
2.5/25.0/2.5	.167	3.28	3.5	0.94
5.0/20.0/5.0	.333	2.57	4.1	0.42
7.5/15.0/7.5	.500	2.40	10.0	0.24
10.0/10.0/10.0	.667	3.06	11.0	0.28
2.5/ 5.0/12.5	.833	3.81	9.5	0.40
13.75/ 2.5/13.75	.917	3.89	5.0	0.78

The shock structure observed with steel/Lucite shields is essentially the same as that for the tungsten/Lucite shields with somewhat higher pressure levels. Therefore, pressure history plots are not reproduced here The effect on compression wave characteristics for Lucite/steel/Lucite shields is summarized in Table 3. The pressurization rate is again minimized for about 50 percent Lucite.

Table 3. Compression Wave Characteristics for Lucite/Steel/Lucite Shields

Shield Configuration (mm/mm/mm)	Lucite Fraction	Peak Pressure (GPa)	Rise Time (μs)	Pressurization Rate (GPa/μs)
1.25/27.5/1.25	.083	5.18	1.4	3.70
2.5/25.0/2.5	.167	4.61	2.1	2.20
5.0/20.0/5.0	.333	3.62	5.9	0.61
6.3/17.4/6.3	.420	3.62	7.0	0.52
7.5/15.0/7.5	.500	3.92	8.4	0.47
10.0/10.0/10.0	.667	4.10	6.2	0.67
12.5/ 5.0/12.5	.833	3.90	5.8	0.67
13.75/ 2.5/13.75	.917	3.43	5.0	0.69

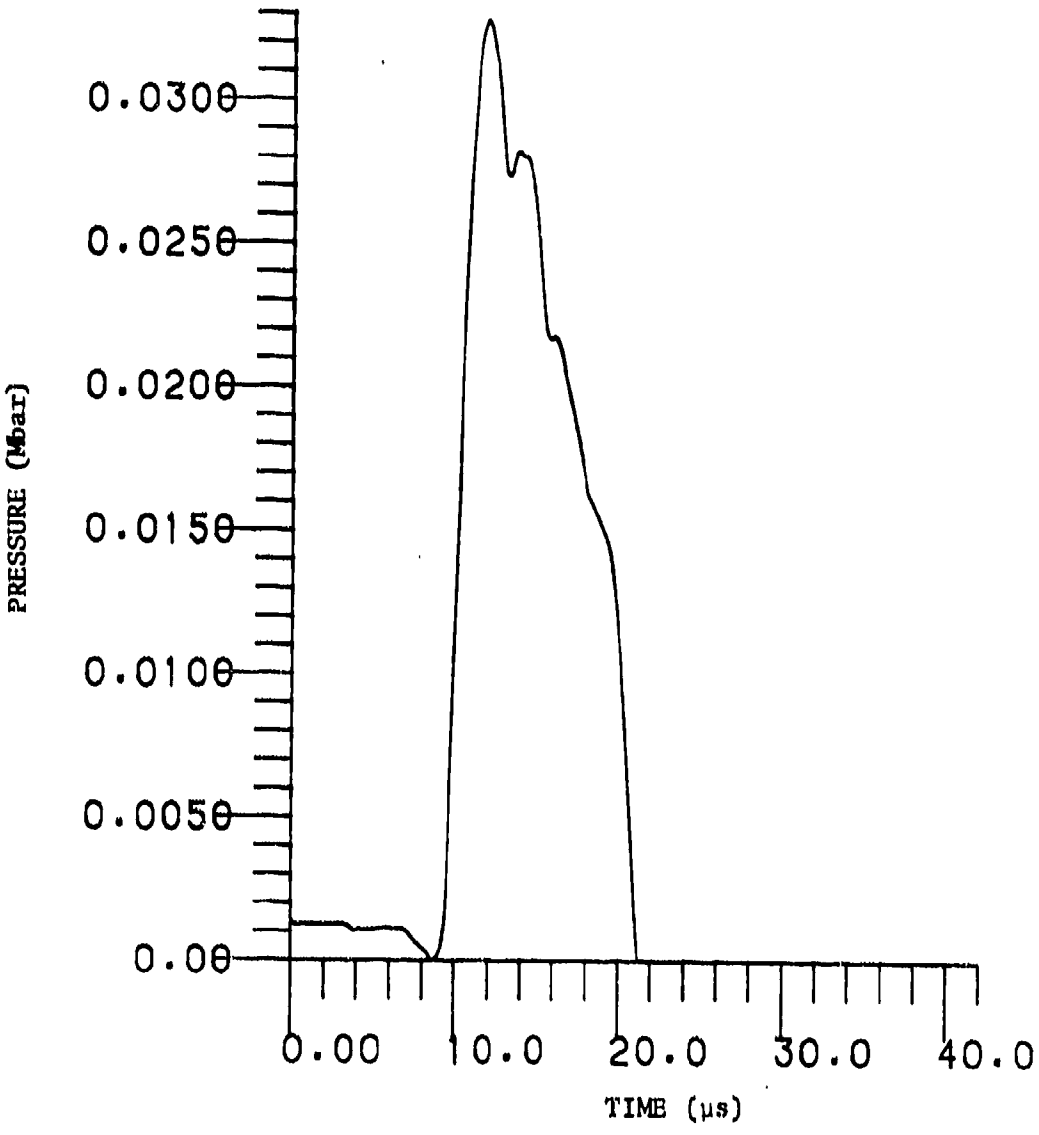

Figure 11a. Acceptor Explosive Pressure History with 30-mm Thick Three-Layered Lucite/Tungsten/Lucite Shield at 16.7% Lucite

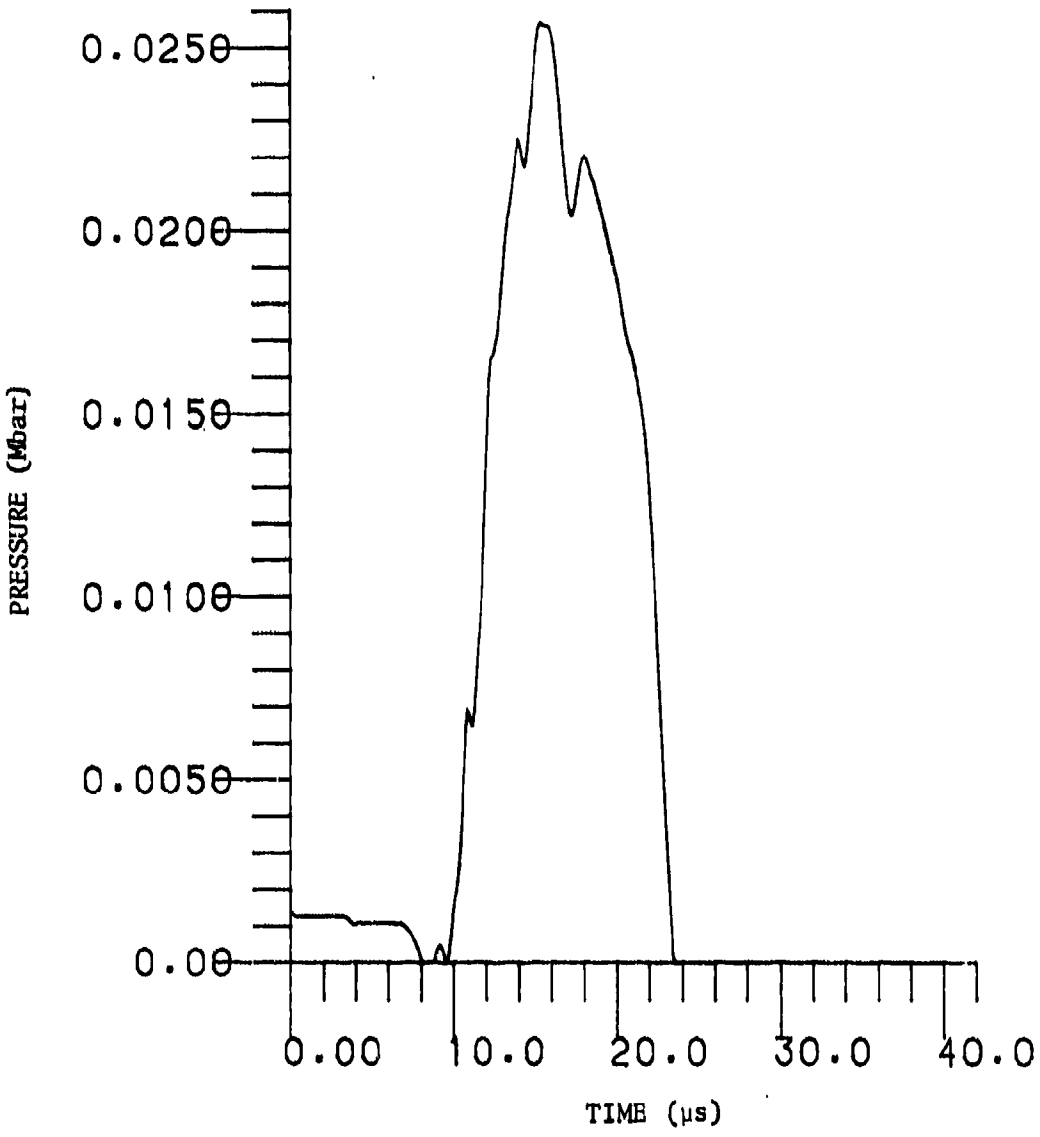

Figure 11b. Acceptor Explosive Pressure History with 30-mm Thick Three-Layered Lucite/Tungsten/Lucite Shield at 33.3% Lucite

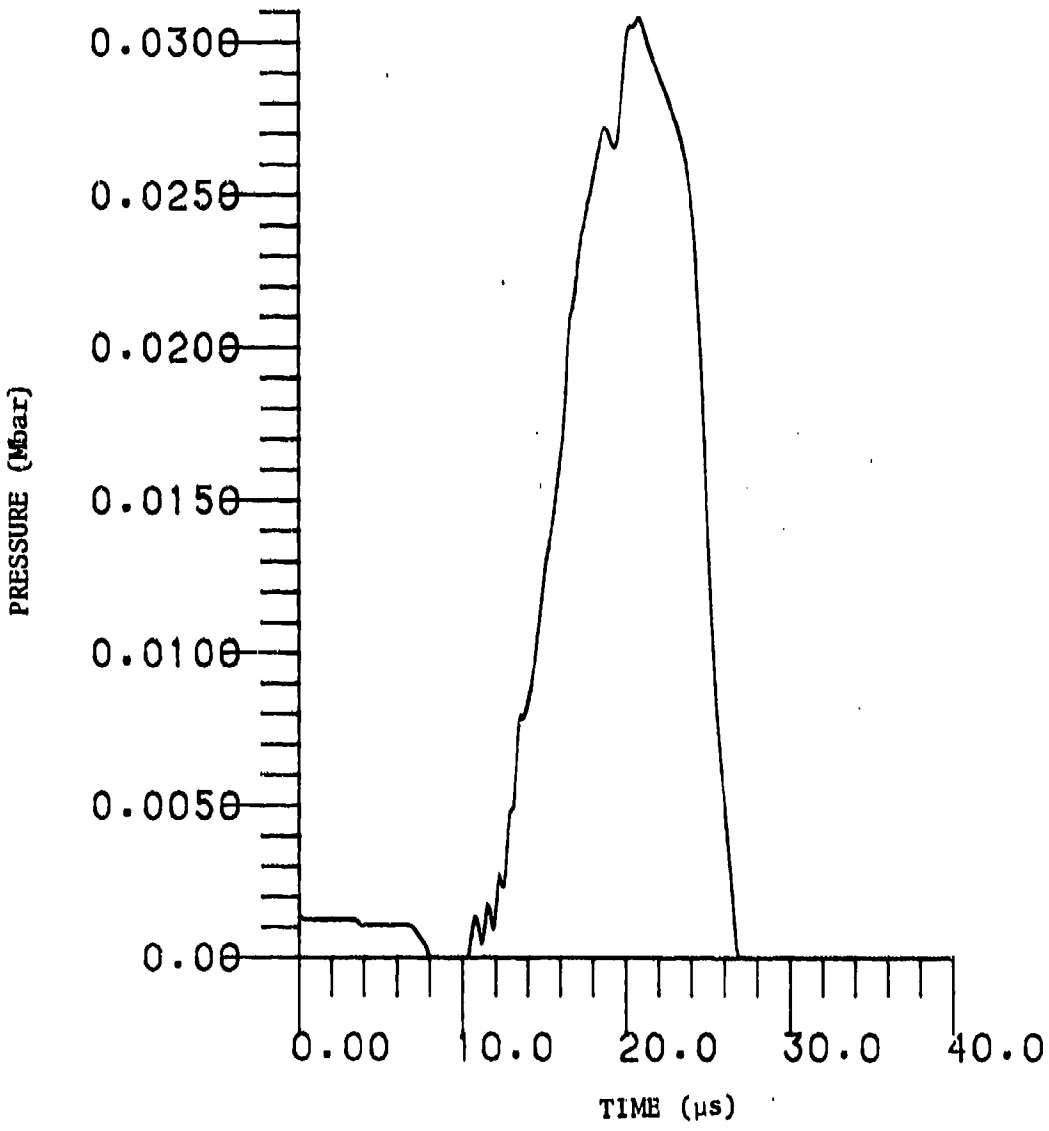

Figure 11c. Acceptor Explosive Pressure History with 30-mm Thick Three-Layered Lucite/Tungsten/Lucite Shield at 66.7% Lucite

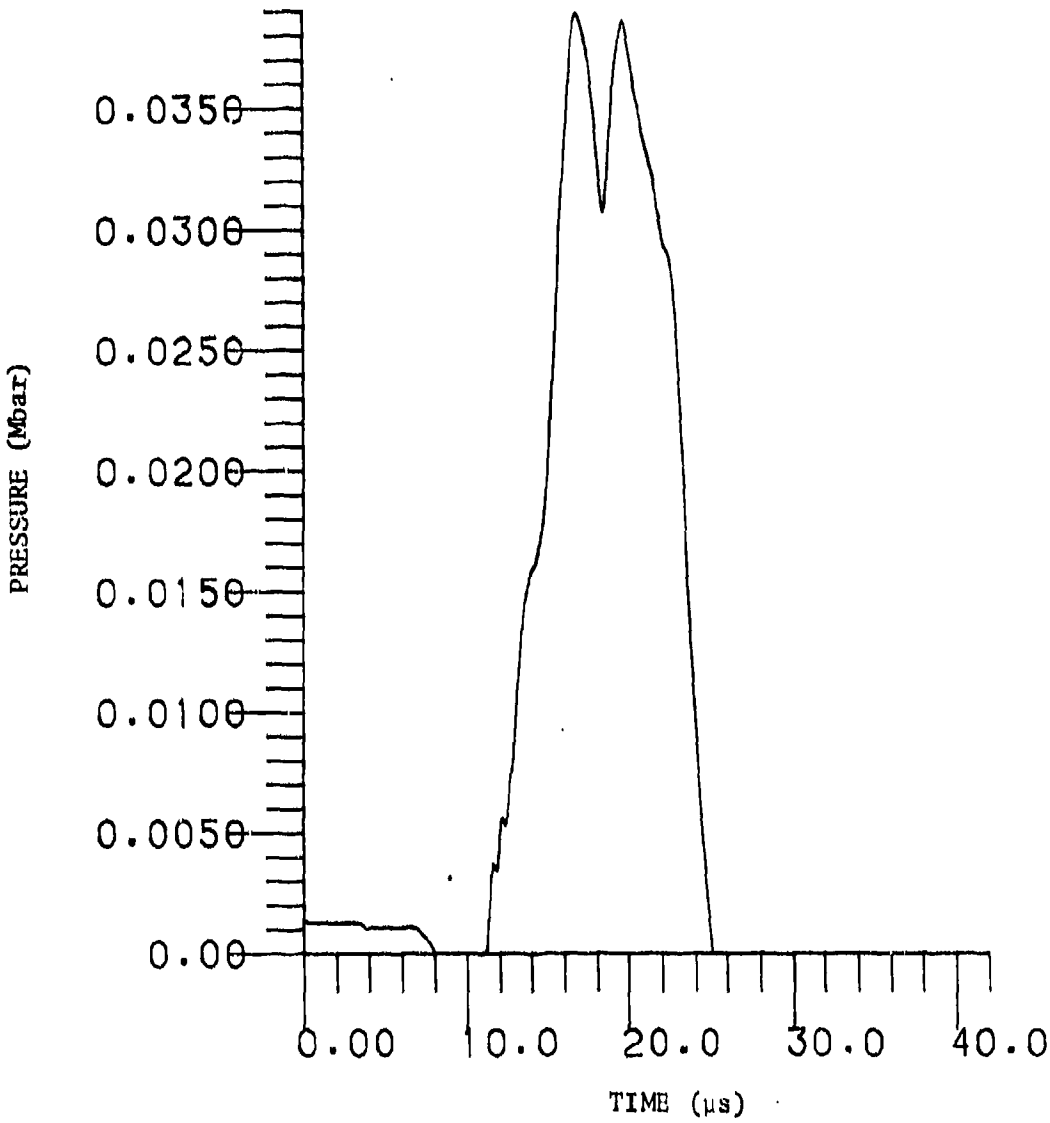

Figure 11d. Acceptor Explosive Pressure History with 30-mm Thick Three-Layered Lucite/Tungsten/Lucite Shield at 91.7% Lucite

Increasing shield thickness has considerable effect on shock breakup. This is illustrated in Figure 12 for 15, 25, 35, and 45 mm thick three-layered shields having tungsten as the outer component. Thin shields produce no breakup, presumably because the close spacing between impedance discontinuities produces closer temporal spacing between shocks leading to rapid coalescence. Figure 12a, for a 15 mm thick shield, seems to show shocks which have just coalesced resulting in a compression wave with a higher rise time. On the other hand, Figure 12d, for a 45 mm thick shield, shows the most shock breakup and peak pressure reduction we have seen in any of our computations.

Five-layered shields produced considerably less shock breakup than three-layered shields of the same thickness, both having tungsten as the outer component. This can be seen by comparing Figure 10d, for a 50 percent Lucite three-layered shield, with Figure 13, for a 50 percent Lucite five-layered shield. Again this presumably occurs because of the closer spacing between impedance discontinuities. This five-layered shield does produce a rise time of 6 to 7 ms.

C. Initiation Stimulus Reduction

Consideration of stimulus levels as characterized by $\int p^2 dt$ allows a comparison of the effectiveness of these shields. Figure 14 is a plot of the relative stimulus level ($\int p^2 dt$ normalized with respect to the value for the unshielded case) versus Lucite thickness fraction for tungsten/Lucite/tungsten and Lucite/tungsten/Lucite shields. Also included are scales of Lucite weight fraction and areal density. This comparison also shows that considerably better shield performance is obtained when tungsten is the outer component of the "sandwich." In fact, the performance of Lucite/tungsten/Lucite shields is inferior to that of either pure tungsten or pure Lucite except for a range of Lucite thickness fraction values between about 0.2 and 0.6 wherein performance is only a little better. It should be noted that this comparison is based on $\int p^2 dt$ and does not take into account the differences between the ramp compressions produced when Lucite is the outer component and the shock breakup and lower peak pressure produced when tungsten is the outer component. Indeed, the response of explosives to these complex waveforms is not well understood and experimental verification is required to determine which shield configuration is superior. However, it should be remarked that the predicted advantage of shields with tungsten on the outside is substantial.

Similar observations may be made for three-layered steel/Lucite shields as shown in Figure 15. The performance of tungsten/Lucite/tungsten shields is compared with that of steel/Lucite/steel shields in Figure 16. This shows that shields incorporating tungsten reduce the initiation stimulus to levels well below those produced by shields incorporating steel.

Shield thickness was varied in two different ways. Shields were varied from 10 to 50 mm in thickness with a constant 50 percent Lucite fraction in one case and from 20 to 50 mm with a constant 7.5 mm outer tungsten layer thickness in the other. The results are plotted versus shield thickness in Figure 17. This shows little difference between the two types of variation and indicates a rapid decline in protection for shields less than about 30 mm thick.

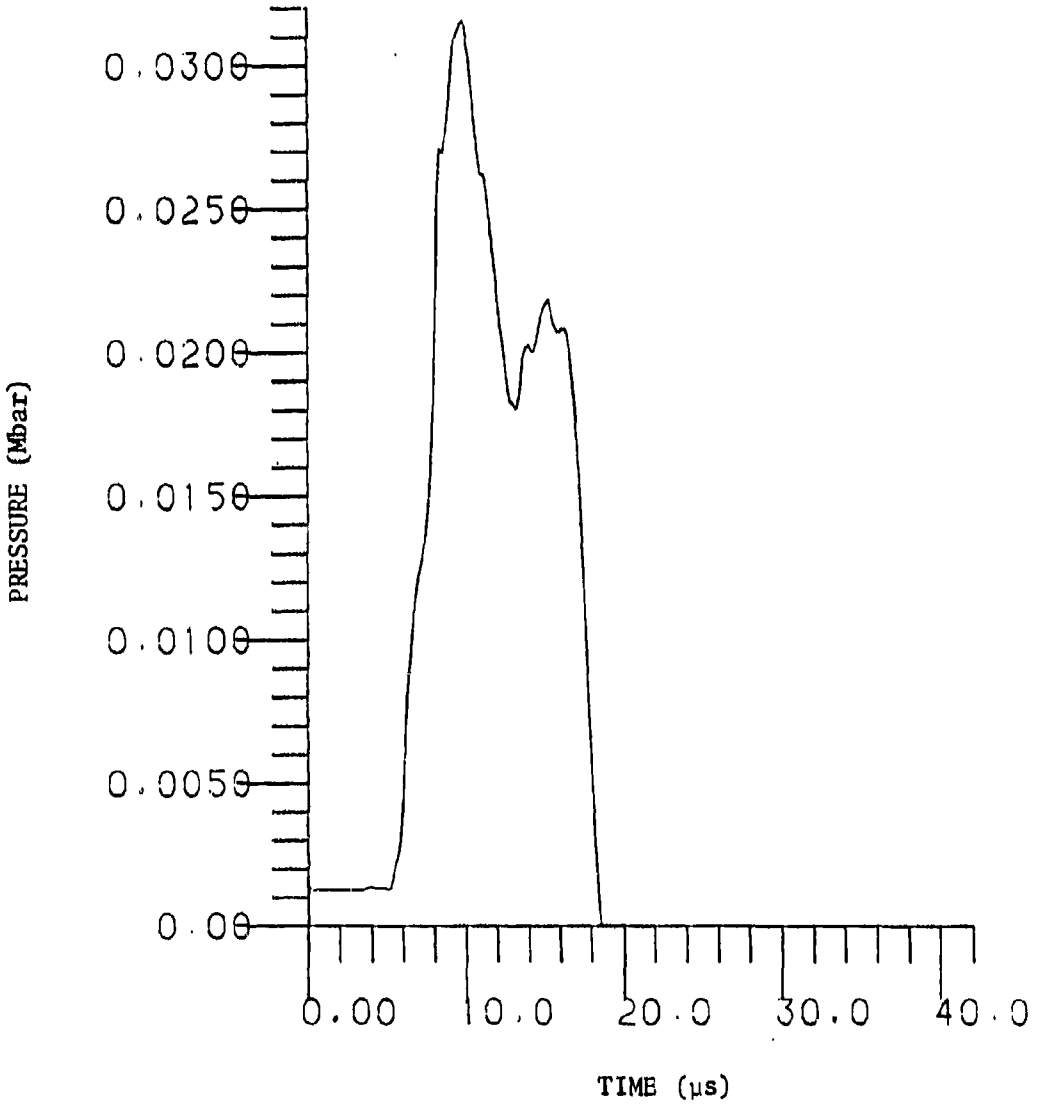

Figure 12a. Acceptor Explosive Pressure History with 50% Lucite Three-Layered Tungsten/Lucite/Tungsten Shields at 15-mm Shield Thickness

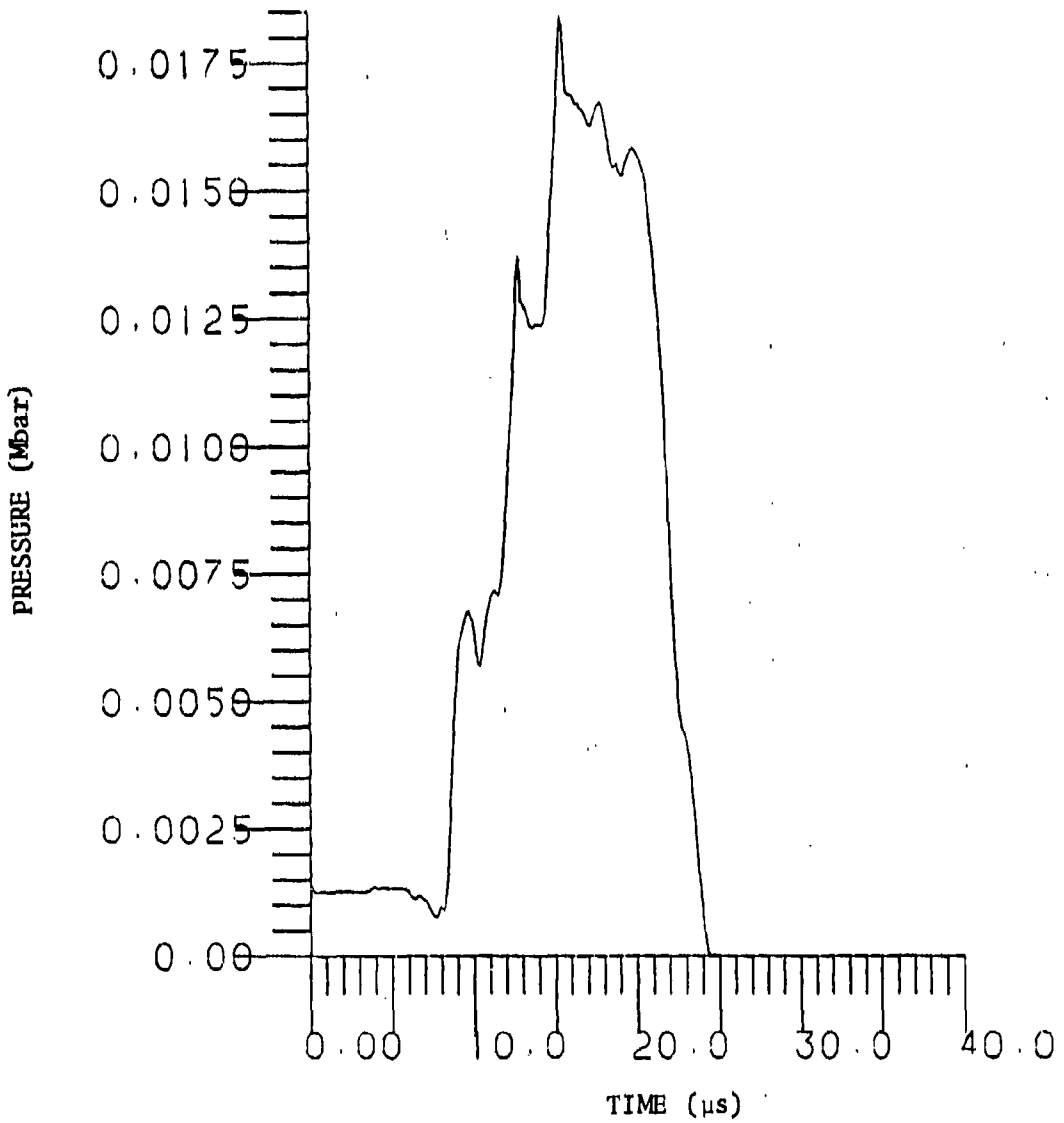

Figure 12b. Acceptor Explosive Pressure History with 50% Lucite Three-Layered Tungsten/Lucite/Tungsten Shields at 25-mm Shield Thickness

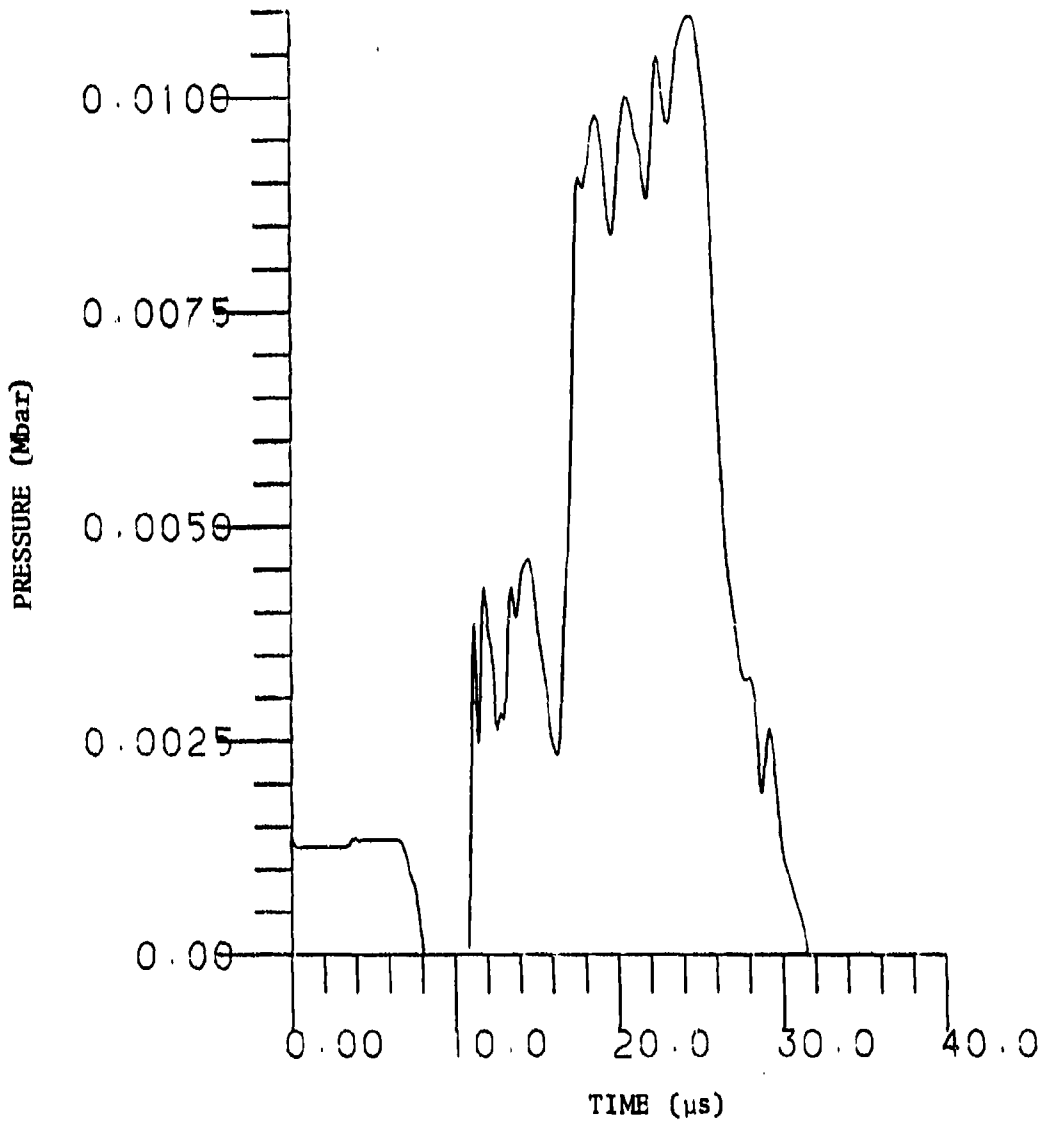

Figure 12a. Acceptor Explosive Pressure History with 50% Lucite Three-Layered Tungsten/Lucite/Tungsten Shields at 35-mm Shield Thickness

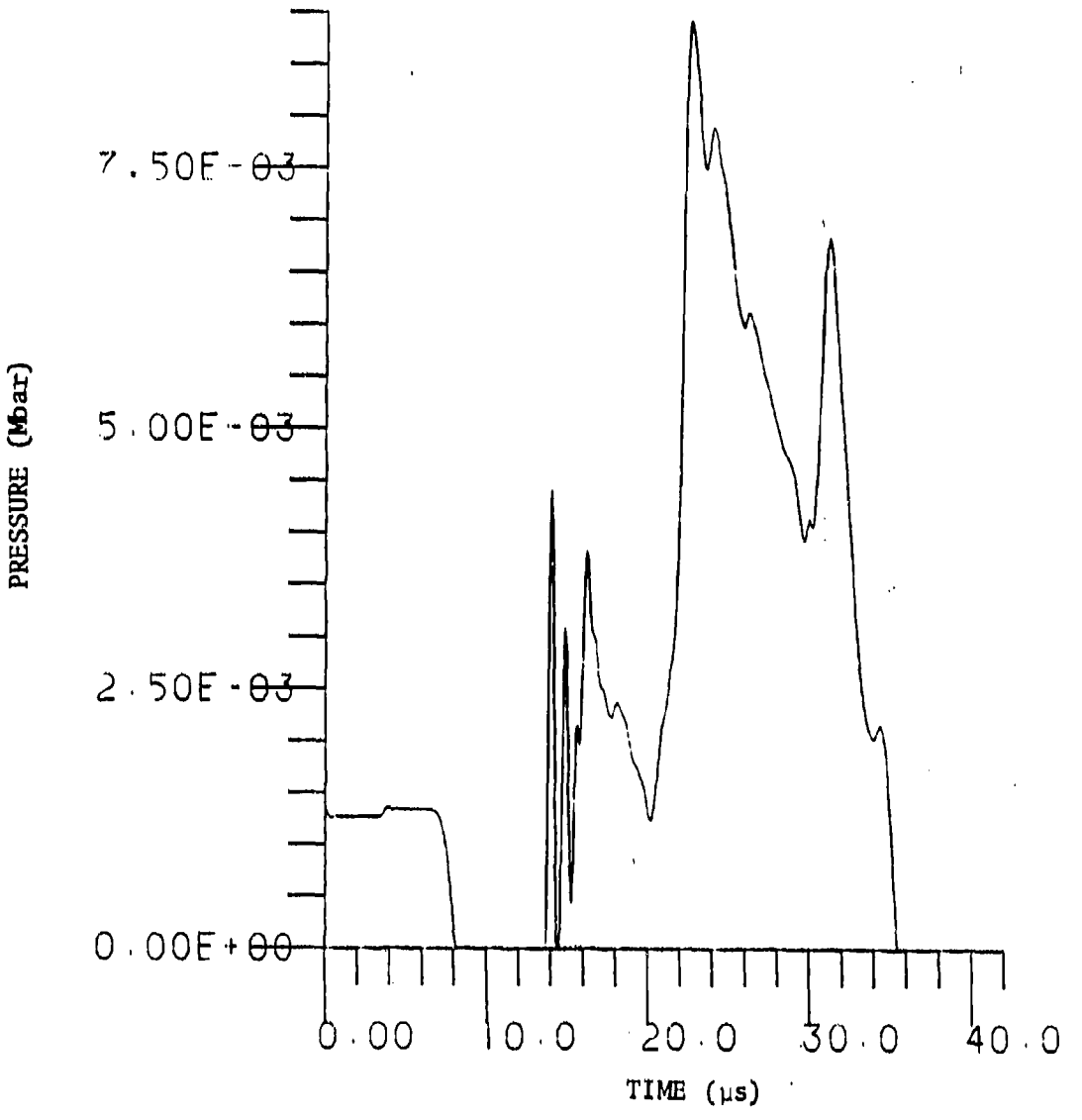

Figure 12d. Acceptor Explosive Pressure History with 50% Lucite Three-Layered Tungsten/Lucite/Tungsten Shields at 45-mm Shield Thickness

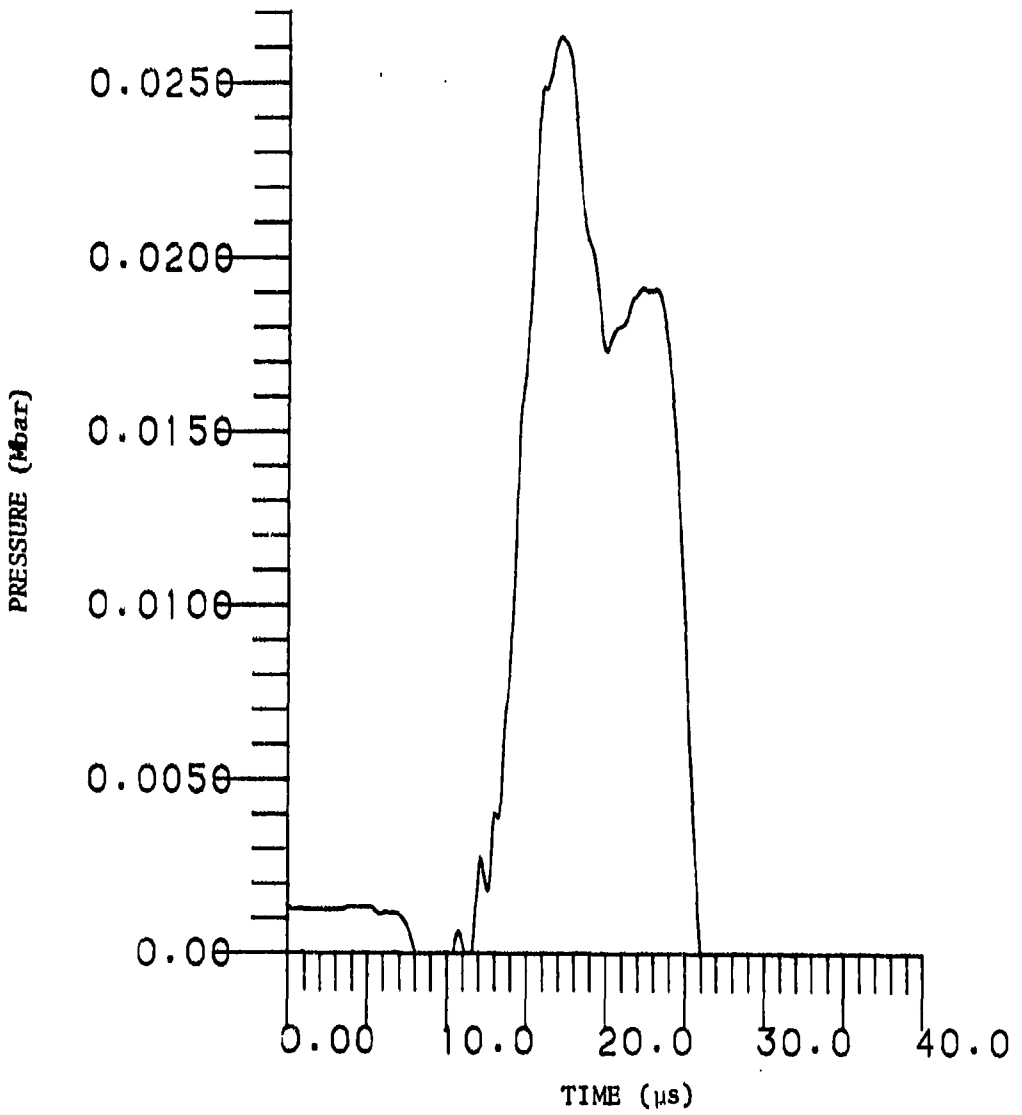

Figure 13. Acceptor Explosive Pressure History with a 30-mm Thick, 50% Lucite Five-Layered Tungsten/Lucite/Tungsten/Lucite/Tungsten Shield

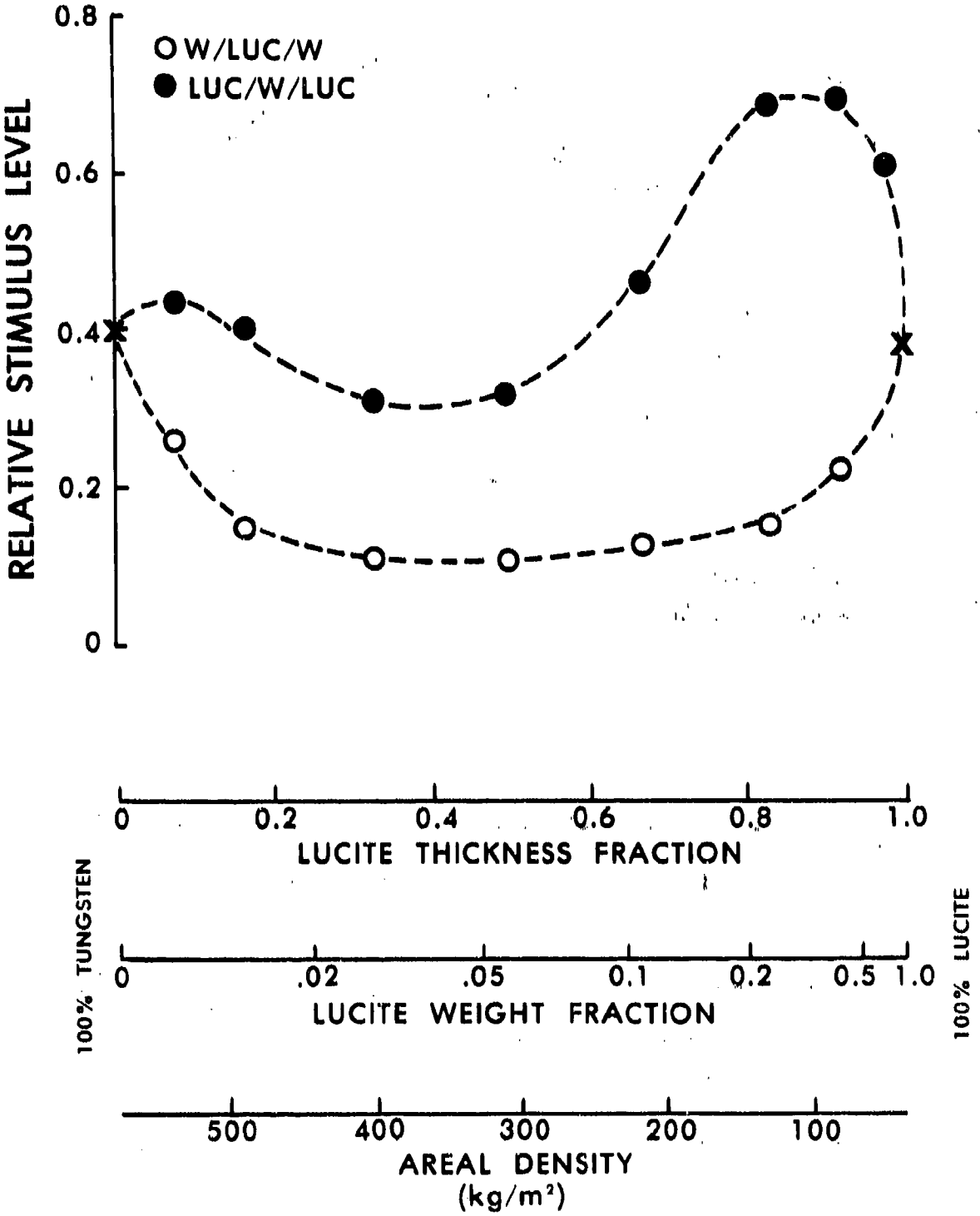

Figure 14. Relative Stimulus Levels for 30-mm Thick, Three-Layered Tungsten/Lucite Shields

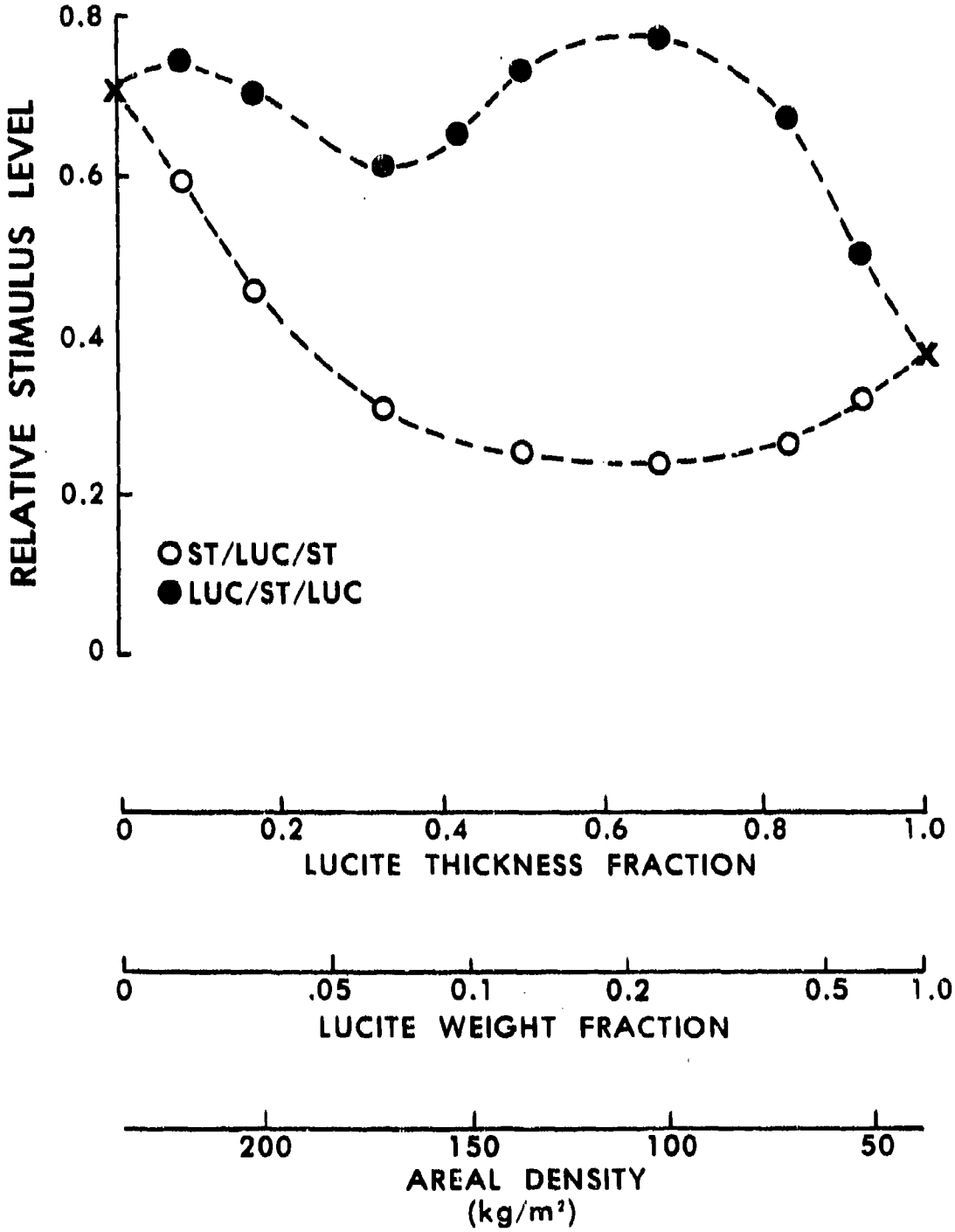

Figure 15. Relative Stimulus Levels for 30-mm Thick, Three-Layered Steel/Lucite Shields

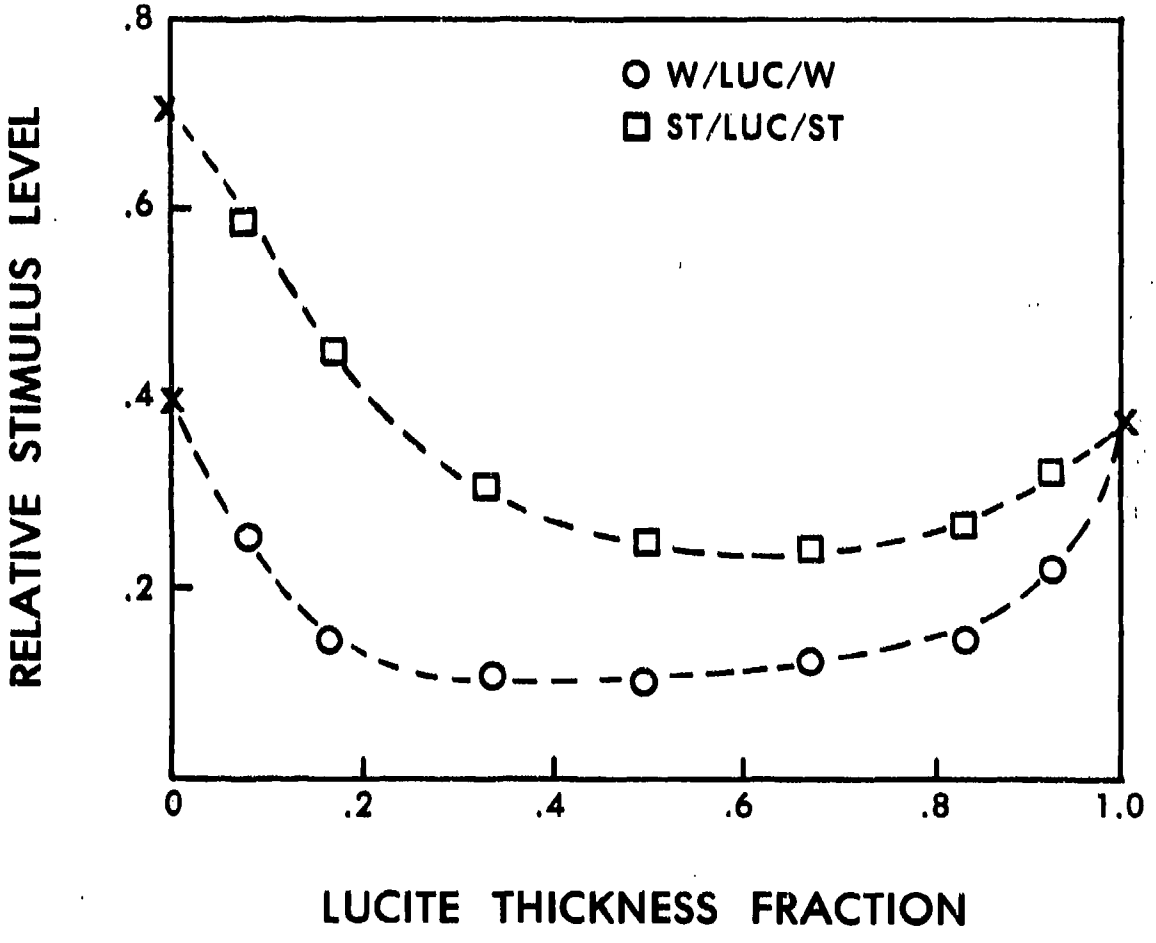

Figure 16. Comparison of Relative Stimulus Levels for 30-mm Thick, Three-Layered Tungsten/Lucite and Steel/Lucite Shields

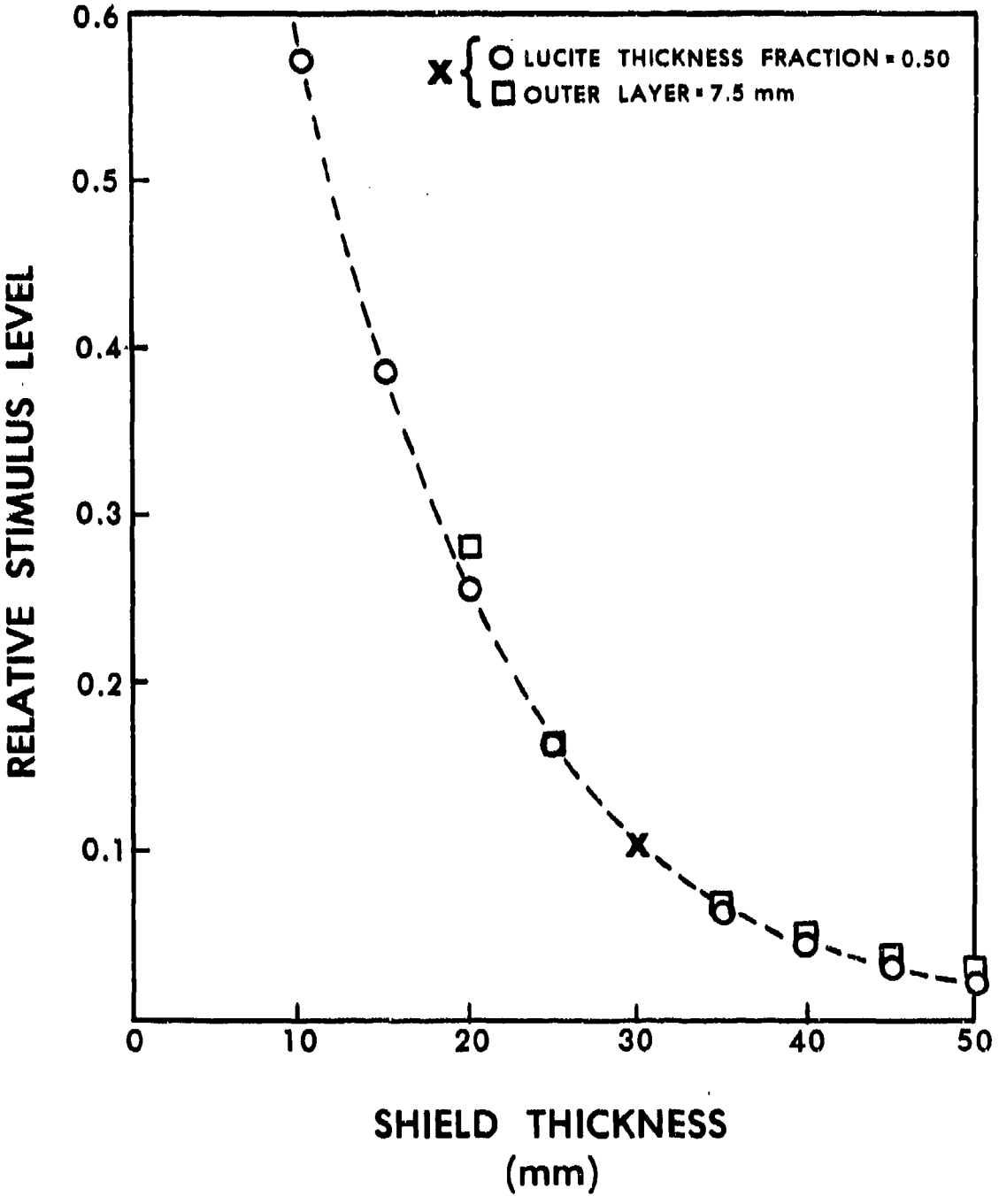

Figure 17. Effect of Shield Thickness on Relative Stimulus Level for Three-Layered Tungsten/Lucite/Tungsten Shields

Results with five-layered shields were similar to those for three-layered shields but not as much protection was provided. We first considered shields with inner and outer layers of equal thickness ($h_i=h_o$). Figure 18 shows the comparison between shields with tungsten on the outside and shields with Lucite on the outside. Again, the former perform better but only slightly better than single layered shields. Figure 19 shows the comparison between the best three-layered shields and the five-layered shields. The three-layered shields are substantially better. The performance of the five-layered shields with tungsten as the outer component is not strongly dependent on Lucite fraction. It is of interest to determine whether shields with unequal inner and outer layer thicknesses perform any better. We noted previously that the parameter z could be used as a measure of the relationship between these layers and that z=0 and $z=h_i/h$ correspond to three-layered shields. We fixed the Lucite thickness fraction at 0.33 and varied z between these limits. The results, shown in Figure 20, indicate a nonmonotonic variation between the two three-layered cases. The three-layered shield with tungsten on the outside still shows the best performance.

VII. SUMMARY

We have conducted a study of the role of shielding in reducing the shock initiation stimulus for a simple one-dimensional representation of the problem of sympathetic detonation of munitions. We found that single layered shields made of materials with low acoustic impedance generally produce a complex shock wave structure in the acceptor. This complex structure is associated with a low level of initiation stimulus because of the breakup into several weaker shocks and the reduction of $\int p^2 dt$. High impedance shield materials also substantially reduce the initiation stimulus, but without the accompanying shock breakup effect. Increasing shield thickness improves performance and can change the order of effectiveness of shield materials. With multi-layered shields composed of a high-impedance and a low-impedance material we observed shock structures depending strongly on the ordering of the materials in the shield. Multiple shock structure was usually observed when the high-impedance material was the outer component of the shield and sufficient low-impedance material was present. Single compression waves with variable peak pressures and rise times were usually observed when the low-impedance material was the outer component of the shield. Substantial benefits in terms of shock breakup and $\int p^2 dt$ reduction can be obtained by increasing the thickness of three-layered shields, which were found to perform better than five-layered shields.

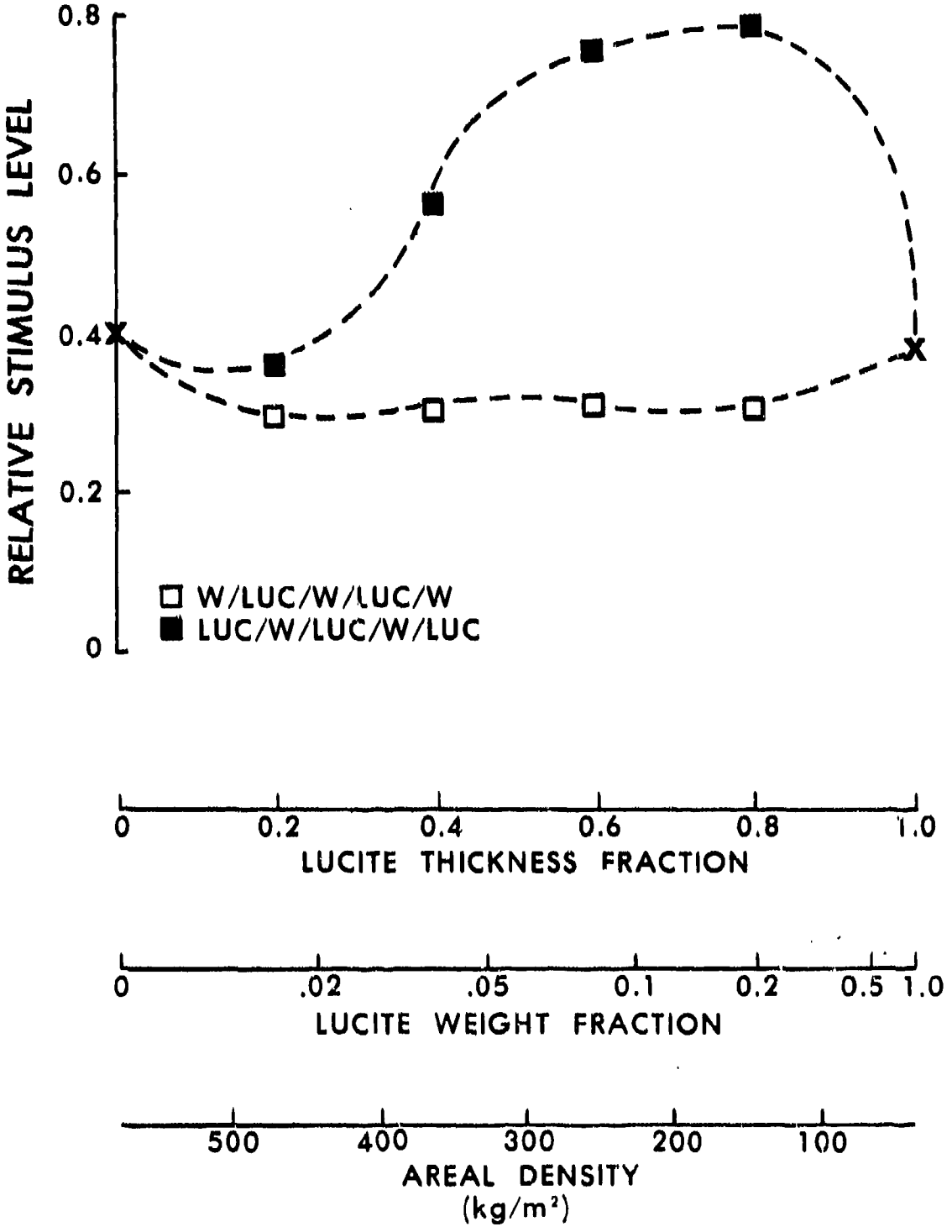

Figure 18. Relative Stimulus Levels for 30-mm Thick, Five-Layered Tungsten/Lucite Shields

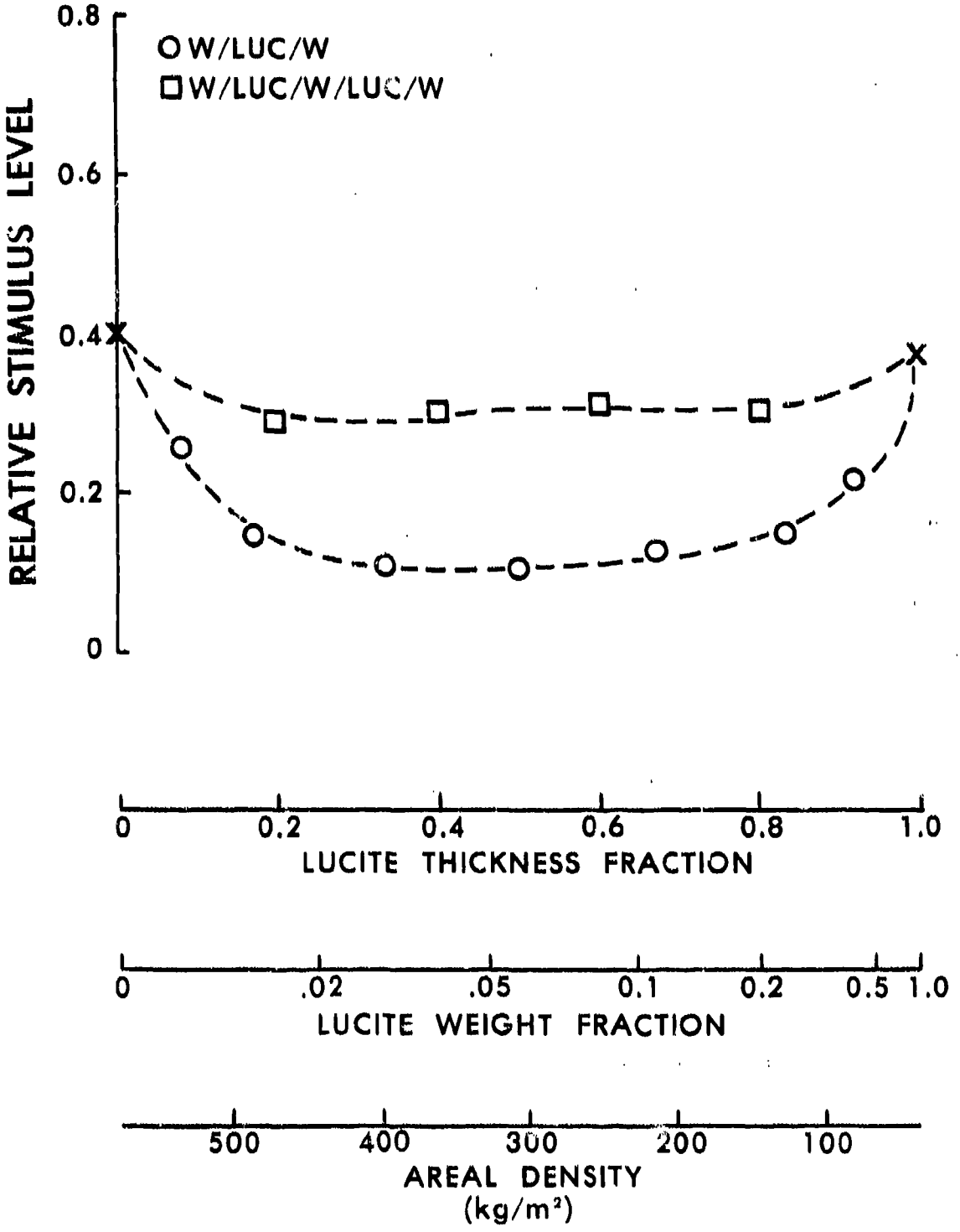

Figure 19. Comparison of Relative Stimulus Levels for 30-mm Thick, Three-Layered and Five-Layered, Tungsten/Lucite Shields

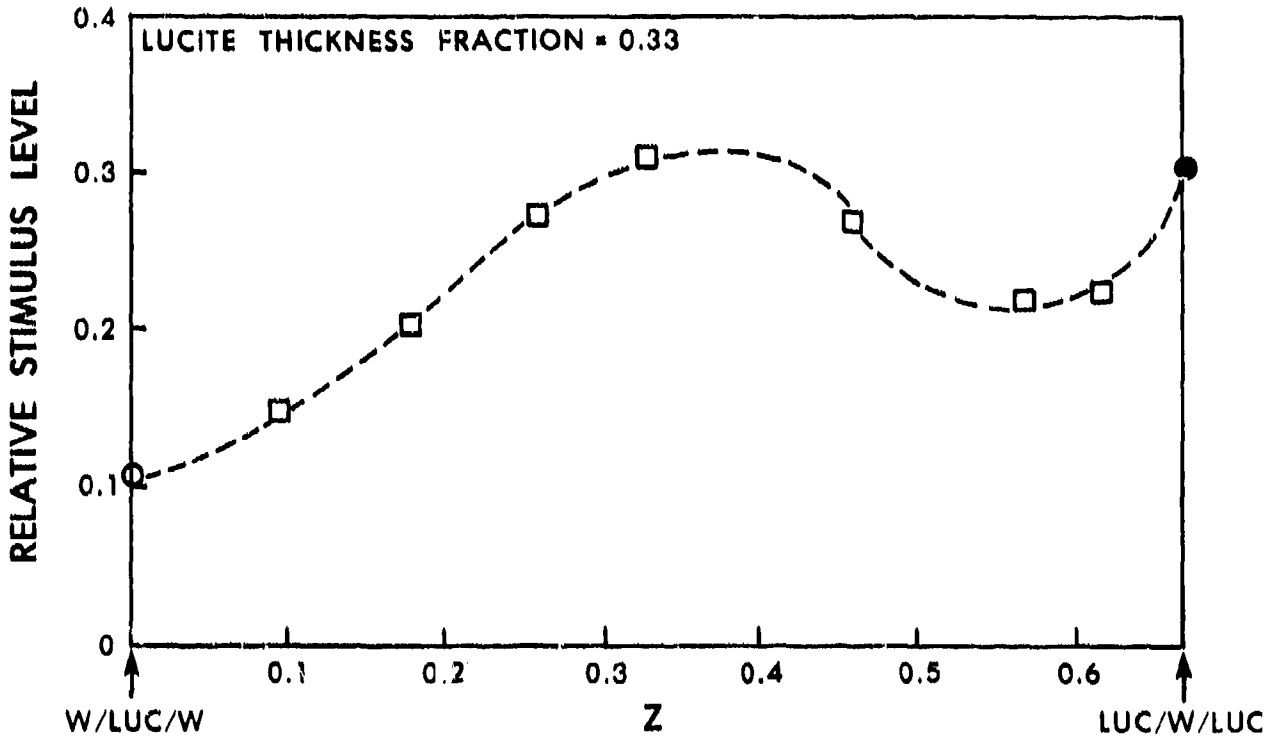

Figure 20. Effect of Shield Configuration on Relative Stimulus Level for 33.3% Lucite, Three-Layered and Five-Layered Shields

DISTRIBUTION LIST

No. of Copies	Organization
12	Administrator Defense Technical Info Center ATTN: DTIC-DDA Cameron Station Alexandria, VA 22304-6145
1	HQDA DAMA-ART-M Washington, DC 20310
2	Chairman DOD Explosives Safety Board ATTN: Dr. T. Zaker COL O. Westry Room 856-C Hoffman Bldg 1 2461 Eisenhower Avenue Alexandria, VA 22331
1	Commander U.S. Army Materiel Command ATTN: AMCDRA-ST 5001 Eisenhower Avenue Alexandria, VA 22333-0001
1	Commander Armament R&D Center US Army AMCCOM ATTN: SMCAR-TDC Dover, NJ 07801-5001
1	Commander Armament R&D Center US Army AMCCOM ATTN: SMCAR-TSS Dover, NJ 07801-5001
1	Commander Armament R&D Center US Army AMCCOM ATTN: SMCAR-LCE, Dr. R. F. Walker Dover, NJ 07801-5001
1	Commander Armament R&D Center US Army AMCCOM ATTN: SMCAR-LCE, Dr. N. Slagg Dover, NJ 07801-5001
1	Commander Armament R&D Center US Army AMCCOM ATTN: SMCAR-LCN, Dr. P. Harris Dover, NJ 07801-5001
1	Commander US Army Armament, Munitions and Chemical Command ATTN: SMCAR-ESP-L Rock Island, IL 61299
1	Director Benet Weapons Laboratory US Army AMCCOM, ARDC ATTN: SMCAR-LCB-TL Watervliet, NY 12189
1	Commander US Army Aviation Research and Development Command ATTN: AMSAV-E 4300 Goodfellow Boulevard St. Louis, MO 63120
1	Director US Army Air Mobility Research and Development Laboratory Ames Research Center Moffett Field, CA 94035
1	Commander US Army Communications Electronics Command ATTN: AMSEL-ED Fort Monmouth, NJ 07703

DISTRIBUTION LIST

No. of Copies	Organization
1	Commander US Army Electronics Research and Development Command Technical Support Activity ATTN: DELSD-L Fort Monmouth, NJ 07703-5301
1	Commander US Army Missile Command ATTN: AMSMI-R Redstone Arsenal, AL 35898
1	Commander US Army Missile Command ATTN: AMSMI-YDL Redstone Arsenal, AL 35898
1	Commander US Army Missile Command ATTN: AMSME-RK, Dr. R.G. Rhoades Redstone Arsenal, AL 35898
1	Commander US Army Tank Automotive Command ATTN: AMSTA-TSL Warren, MI 48090
1	Director US Army TRADOC Systems Analysis Activity ATTN: ATAA-SL White Sands Missile Range NM 88002
1	Commandant US Army Infantry School ATTN: ATSH-CD-CSO-OR Fort Benning, GA 31905
1	Commander US Army Development & Employment Agency ATTN: MODE-TED-SAB Fort Lewis, WA 98433
1	Commander US Army Research Office ATTN: Chemistry Division P.O. Box 12211 Research Triangle Park, NC 27709-2211
1	Office of Naval Research ATTN: Dr. J. Enig, Code 200B 800 N. Quincy Street Arlington, VA 22217
1	Commander Naval Sea Systems Command ATTN: Mr. R. Beauregard, SEA 64E Washington, DC 20362
1	Commander Naval Explosive Ordnance Disposal Technology Center ATTN: Technical Library Code 604 Indian Head, MD 20640
1	Commander Naval Research Lab ATTN: Code 6100 Washington, DC 20375
1	Commander Naval Surface Weapons Center ATTN: Code G13 Dahlgren, VA 22448
9	Commander Naval Surface Weapons Center ATTN: Mr. L. Roslund, R122 Mr. M. Stosz, R121 Code X211, Lib E. Zimet, R13 R.R. Bernecker, R13 J.W. Forbes, R13 S.J. Jacobs, R10 Dr. C. Dickinson J. Short, R12 Silver Spring, MD 20910

DISTRIBUTION LIST

No. of Copies	Organization
4	Commander Naval Weapons Center ATTN: Dr. L. Smith, Code 3205 Dr. A. Amster, Code 385 Dr. R. Reed, Jr., Code 388 Dr. K.J. Graham, Code 3835 China Lake, CA 93555
1	Commander Naval Weapons Station NEDED ATTN: Dr. Louis Rothstein, Code 50 Yorktown, VA 23691
1	Commander Fleet Marine Force, Atlantic ATTN: G-4 (NSAP) Norfolk, VA 23511
2	Commander Air Force Rocket Propulsion Laboratory ATTN: Mr. R. Geisler, Code AFRPL MKPA Lt. Jann Hoopes Cassady, Stop 24 Edwards AFB, CA 93523
5	Commander Air Force Armaments Technology Laboratory ATTN: M. Zimmer L. Elkins G. Parsons B. G. Craig N. P. Loverro Eglin Air Force Base, FL 32542
1	AFWL/SUL Kirtland AFB, NM 87117
1	Commander Ballistic Missile Defense Advanced Technology Center ATTN: Dr. David C. Sayles P.O. Box 1500 Huntsville, AL 35807
1	Director Lawrence Livermore National Lab University of California ATTN: Dr. M. Finger P.O. Box 808 Livermore, CA 94550
1	Director Lawrence Livermore National Lab University of California ATTN: Dr. R. McGuire P.O. Box 808 Livermore, CA 94550
1	Director Lawrence Livermore National Lab University of California ATTN: Dr. C. Tarver P.O. Box 808 Livermore, CA 94550
1	Director Lawrence Livermore National Lab University of California ATTN: Dr. E. Lee P.O. Box 808 Livermore, CA 94550
1	Director Los Alamos National Lab ATTN: John Ramsey P.O. Box 1663 Los Alamos, NM 87545
1	Director Los Alamos National Lab ATTN: S. Goldstein P.O. Box 1663 Los Alamos, NM 87545
1	Director Los Alamos National Lab ATTN: Dr. C. Mader P.O. Box 1663 Los Alamos, NM 87545

DISTRIBUTION LIST

No. of Copies	Organization
1	Director Los Alamos National Lab ATTN: I. B. Akst P.O. Box 1663 Los Alamos, NM 87545
1	Director Los Alamos National Lab ATTN: Edward Court P.O. Box 1663 Los Alamos, NM 87545
1	Director Sandia National Lab ATTN: Dr. J. Kennedy Albuquerque, NM 87115

Aberdeen Proving Ground

Dir, USAMSAA
ATTN: AMXSY-D
AMXSY-MP, H. Cohen
Cdr, USATECOM
ATTN: AMSTE-TO-F
Cdr, CRDC, AMCCOM,
ATTN: SMCCR-RSP-A
SMCCR-MU
SMCCR-SPS-IL

No. of Copies	Organization
1	Air Force Armament Laboratory ATTN: AFATL/DLODL Eglin AFB, FL 32542-5000

USER EVALUATION SHEET/CHANGE OF ADDRESS

This Laboratory undertakes a continuing effort to improve the quality of the reports it publishes. Your comments/answers to the items/questions below will aid us in our efforts.

1. BRL Report Number _____ Date of Report _____

2. Date Report Received _____

3. Does this report satisfy a need? (Comment on purpose, related project, or other area of interest for which the report will be used.) _____

_____

_____

4. How specifically, is the report being used? (Information source, design data, procedure, source of ideas, etc.) _____

_____

_____

5. Has the information in this report led to any quantitative savings as far as man-hours or dollars saved, operating costs avoided or efficiencies achieved, etc? If so, please elaborate. _____

_____

_____

6. General Comments. What do you think should be changed to improve future reports? (Indicate changes to organization, technical content, format, etc.)

_____

_____

_____

CURRENT ADDRESS

_____
Name

_____
Organization

_____
Address

_____
City, State, Zip

7. If indicating a Change of Address or Address Correction, please provide the New or Correct Address in Block 6 above and the Old or Incorrect address below.

OLD ADDRESS

_____
Name

_____
Organization

_____
Address

_____
City, State, Zip

(Remove this sheet along the perforation, fold as indicated, staple or tape closed, and mail.)

FOLD HERE

Director
US Army Ballistic Research Laboratory
ATTN: AMXBR-OD-ST
Aberdeen Proving Ground, MD 21005-5066

NO POSTAGE
NECESSARY
IF MAILED
IN THE
UNITED STATES

OFFICIAL BUSINESS
PENALTY FOR PRIVATE USE, $300

BUSINESS REPLY MAIL
FIRST CLASS PERMIT NO 12062 WASHINGTON, DC
POSTAGE WILL BE PAID BY DEPARTMENT OF THE ARMY

Director
US Army Ballistic Research Laboratory
ATTN: AMXBR-OD-ST
Aberdeen Proving Ground, MD 21005-9989

FOLD HERE